Hydrodynamics of an Oilwell Blowout

D.R. TOPHAM

Technical Report No. 33

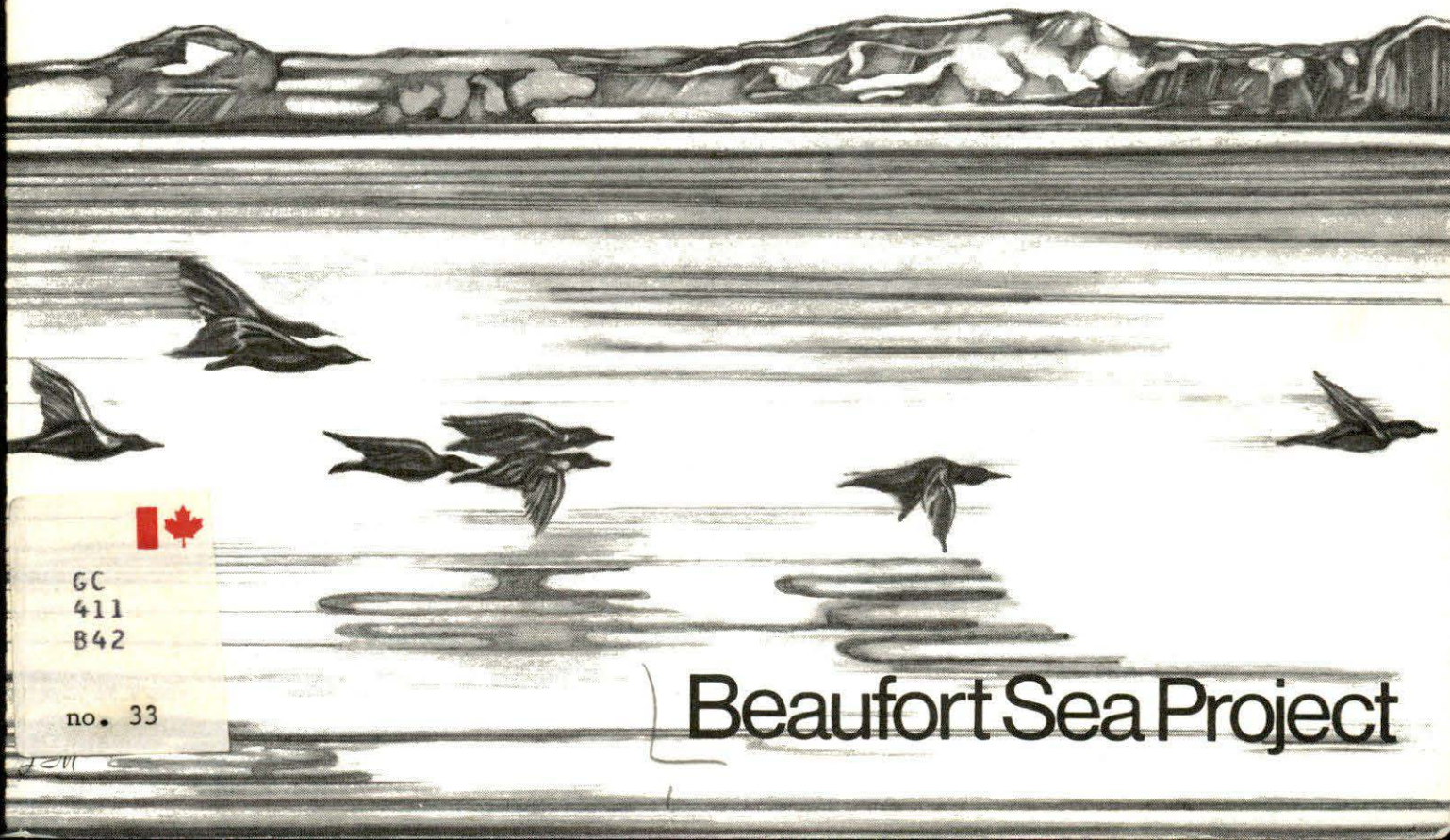

Beaufort Sea Project

HYDRODYNAMICS OF AN OILWELL BLOWOUT

D. R. Topham

Frozen Sea Research Group
Department of the Environment
825 Devonshire Road
Victoria, B.C. V8W 1Y4

Beaufort Sea Technical Report #33

Beaufort Sea Project
Dept. of the Environment
512 Federal Building
1230 Government St.
Victoria, B.C. V8W 1Y4

December, 1975

TABLE OF CONTENTS

1. SUMMARY

Two aspects of an under sea oil well blowout have been investigated experimentally. Firstly a full scale blowout was simulated by pumping the equivalent of up to 27 m^3/min of air at atmospheric pressure down to depths of 60 m and 23 m of seawater and measuring the induced flow patterns. These were similar in all cases, a central rising plume with a surface radial flow at the point of impingement. A striking feature of the radial flow pattern was a ring of waves concentric with the plume centre. This marks a division in the directions of the surface radial currents, outwards within, and inwards beyond the ring. This flow system would provide a certain amount of natural containment for the oil.

Secondly, an experiment was carried out to investigate the possibility of stable emulsions being formed close to the well exit. Mixtures of oil and gas were injected under water with appropriate velocities through a common pipe exit. Two specific oils were used to represent extremes of the types expected in the Beaufort Sea; one was known not to form stable emulsions and the other thought likely to form stable water-in-oil emulsions. In both cases the oil was shattered into droplets within a short distance of the pipe exit, with the major part of the oil in droplets 1 mm in diameter. A small proportion, of the order of 1%, was in droplets of 50 microns or less in diameter.

Most of the oil will reach the surface as 1 mm diameter droplets and be swept radially outwards by the induced surface currents and coalesce on the surface within the wave ring. After a critical depth is exceeded the oil will overcome the retaining flows and collect beyond the wave ring. The smaller drops may be carried down to depths of up to 10 m in the case of a 60 m plume and if released into a current would be carried several kilometers downstream.

2. INTRODUCTION

The rapid expansion of the exploration for oil and gas in the Canadian Arctic with the consequent risk to the environment has led to a large-scale environmental study - the Beaufort Sea Project. Of prime concern are the environmental risks attendant on an uncontrolled oil well blowout on the sea bed in ice covered waters. To assess this problem a 'standard Beaufort Sea blowout' was agreed upon as that expected from the geological formations of the area. This is as follows: an initial oil flow rate of 2500 barrels/day (398 m^3/day) decaying linearly to 1000 barrels/day (159 m^3/day) after one month and then continuing at this rate indefinitely or until plugged. The oil contains dissolved gas within the reservoir in an amount equal to 22.7 m^3/barrel when expanded to atmospheric pressure.

The work described in this report concerns the behaviour of the oil/gas mixture as it leaves the pipe exit, its transport to the sea surface, and the locally induced water flows. A preliminary appraisal of this problem based on existing information on rising bubble plumes revealed a lack of knowledge of the behaviour of such systems on the scale of the projected oil well blowout (Topham 1974), and the experiments reported here were undertaken to obtain data under full scale conditions.

Two separate experiments were undertaken, a full-scale simulation of the gas bubble plume in 60 m of seawater using air compressors, and a tank experiment investigating the behaviour of gas/oil mixtures at an underwater pipe exit. As these two experiments were separate investigations, they are presented as self-contained sections and the major consequences are delineated in a separate section describing a probable blowout scenario.

3. SIMULATION OF AN OIL WELL BLOWOUT IN SHALLOW COASTAL WATERS

2.1 Selection of Test Conditions

It is anticipated that exploratory drilling will take place in water ranging between 15 m and 180 m in depth. The standard Beaufort Sea blowout detailed in the introduction yields an initial gas volume flow of 39 m^3/min of gas at atmospheric pressure, and the experiment was designed to duplicate these conditions as closely as possible.

Bubble plumes have been studied by a number of workers, although more frequently for the case of a 2-dimensional line source of bubbles. Such systems find practical application as breakwaters (Bulson 1961), and as a means of mixing salt and fresh water to prevent freezing, (Carstens 1971). A comprehensive review of this literature has been given by Jones (1972) and the application of axisymmetric plumes to the oil well blowout discussed by the present author (Topham 1974), and to ice melting by Ashton (1974). The mathematical modelling of such plumes is based on the analogy between density deficiency due to heat, and that due to the presence of the distributed bubbles throughout the water column. None of the theoretical models so far applied to bubble plumes have considered the expansion of the gas bubbles during their ascent. It has been pointed out by Turner (1973) that this can be treated in the same manner as a plume of constant total buoyancy in an ambient fluid of changing density; the significant factor is the buoyancy difference between the plume and its surroundings. Experimental results reported in the literature are restricted to water depths and gas flow rates far below those of the anticipated oil well blowout. Maximum depths and flow rates reported are 4.5 m and 0.36 m^3/min for axisymmetric plumes by Kobus (1968), and 10 m and 9.3 m^3/min/m for a 2-dimensional plume by Bulson (1961).

The gas flow rates and depths of the projected well blowout, 39 m^3/min of free gas and 180 m are an order of magnitude greater than previous experiments, and the present work was undertaken to provide information under near full-scale conditions.

Air was substituted for natural gas, as its solubility in water is close to that of methane, the major constituent of natural gas, allowing conventional high capacity air compressors to be used. It was not practical to perform the experiment under ice or to provide a solid sea cover over a large enough area, but it is believed that the broad features of the resulting flow patterns will be similar and can be derived from the open water case.

2.2 Experimental Layout

Air was supplied from two 200 kw rotating screw compressors having a nominal maximum total delivery of 50 m^3/min of free air at a supply pressure of 7.8 atmospheres. This supply pressure determined the maximum working depth of the discharge nozzle as 60 m. Two sites were chosen in Saanich Inlet, Vancouver Island, one with a sea bed depth of 73 m with the discharge nozzle at 60 m and the other with the discharge nozzle on the sea bed at 23 m depth.

A 3.7 m sq. raft moored above the nozzle outlet served as a suspension platform for a 12 m horizontal beam carrying 20 Savonius rotors mounted to measure flow speeds in the vertical plane. A steel cable between the raft and the sea bed served to locate the discharge nozzle and also as a guide for the instrument carrying beam. Additional surface mooring lines provided the means to centre the raft over the plume, Figure 2.1. Radial profiles of the vertical flows were obtained by lowering the beam down the guide wire, recording the rotor speeds by means of electro-mechanical counters and stopwatch. The horizontal current strengths and directions away from the central plume were measured with a single current meter suspended from a small boat moored at various radial positions along the surface mooring lines. Vertical profiles of the water temperature and density both before the plume was started and at various positions around the established plume were measured with a Guildline Model 8101A CTD unit. Additional information on the plume structure was obtained from a vertically oriented side-scan sonar system.

2.3 Results

2.3.1 60 m depth

Measurements were made on plumes having flow discharges of 11, 22, and 26.6 m^3/min of free air and of one at a slightly reduced depth of 53 m with a discharge rate of 27.6 m^3/min. The general features of the induced flow pattern were similar in all cases, consisting of a central rising plume with a surface radial flow as it impinged on the surface. A striking feature of the radial flow pattern was a ring of waves concentric with the plume centre. This marked a division in the direction of the radial surface currents, outwards within, and inwards beyond the ring. This flow system forms a natural capture area for floating debris in the vicinity. The surface flows were not steady, but contained large scale fluctuations arising from eddies within the central plume After impinging on the surface, these spread rapidly as expanded vortices, coming to a halt at the wave ring radius which marks the complex interaction region where the fluid mixes downwards. This downward mixing entrains the inwards directed flow outside the ring. The side scan sonar records suggest that some bubbles are carried out to the wave ring and are mixed down to a depth of 12 m in an annular ring positioned below the wave ring.

A series of velocity profiles was obtained from each depth, each being based on a one-minute integration period of the meter revolution counters. Six consecutive counting periods were monitored, each separated by about 30 seconds required to record the readings; the curves shown are the means of all six of these one-minute integration periods. The individual velocity profiles were irregular in shape and the position of the maximum velocity relative to the mean profile centerline varied considerably. It is difficult to separate such variations from those arising from lateral movement of the surface raft and its mooring system. Such motions, however, would tend to exaggerate the plume radius towards the surface and increase the apparent angular divergence of the plume. It was not practical to measure velocity profiles with more than one radial orientation of the instrument boom and the profiles do not account for any asymmetry due to cross currents although measurements of these before the plume was started showed them to be negligible in most cases.

The central plumes were initially conical in shape, but after rising to a height of roughly 23 m the radius remained approximately constant with a further expansion approaching the surface. The centerline velocity decreases with height as the plume diameter increases, and changes little over the remainder of the plume height. The distributions of plume radius and centerline velocity with height are shown in Figures 2.2 to 2.5, where the radius has been defined as that at which the velocity has fallen to 15% of the centerline value. This rather large value was chosen to minimize errors accumulated on the current meters from the transmission of surface wave action to the instrument mounting boom.

The mean velocity proviles for the 11.0 m^3/min and 22 m^3/min flows at 60 m depth are shown in Figures 2.6 and 2.7 and for the 27.6 m^3/min flow at 53 m depth in Figure 2.8.

These velocity profiles show little similarity with changing depth and the changes in plume shape from conical to cylindrical suggest some change in plume development mechanisms. This is better illustrated in Figure 2.9 which shows the variation of total mass flow in the plume with height from the source for different flow rates. These all show marked irregularities with distinct reductions in gradient, a measure of the rate of entrainment of fluid. Figure 2.10 shows the mean profiles of radial velocity near the surface away from the plume centerline. These clearly show the reversal of surface current beyond the wave ring radius.

Density and temperature profiles taken before starting the plume revealed a cold layer of low salinity roughly 9 m deep overlying the main body of water, Figure 2.11. Profiles taken with the established plume showed strong mixing of the surface layer to have occurred within the wave ring, Figure 2.12, whilst the profiles outside remained unchanged.

2.3.2 23 m depth

Three airflow rates, 3.6 m^3, 29.2 m^3 and 40 m^3 of free air per minute were studied in detail at this depth, whilst visual observations were made of a flow of 62 m^3/min, the latter producing such a violent interaction with the surface that the raft became unstable. At this large flow rate surface eruptions of foam up to 1 metre in height were observed. Figures 2.13, 2.14, and 2.15 show these results, the lowest flow rate giving a conical plume with constant centerline velocity, whilst at the higher flows the plume expanded more rapidly, with a sudden expansion in diameter occurring at a height of 12 m.

These flows produced surface features similar to those of the 60 m case, with a reduced radius for the wave ring 20 m in the case of the 40 m^3/min flow. This radius was a weak function of air flow rate, reducing to about 9 m for the 3.6 m^3/min flow.

2.4 Discussion

The significant differences between these plumes and those reported in the literature are the high air injection rates and the large changes in buoyancy due to the expansion of the rising bubbles. The latter are shown in Figures 2.16 and 2.17 for the two test depths, calculated on a simple pressure-volume basis. As noted in the introduction, the effect of changing buoyancy can be treated in the same manner as a variable ambient density, and in principle the heated plume analogy can be extended to the deep bubble plume. However, this analogy requires that the bubbles be small, so that their natural rise velocity is small compared with local fluid velocities. Observations of the size of the bubbles using an underwater TV camera showed that this requirement was not met by a considerable fraction of the air volume. The larger bubbles ranged roughly from 1.5 cm to 3 cm in diameter with separations of several centimeteres. Single bubbles of this size would have terminal velocities of 30 to 60 cm/sec. (Datta et al, 1950).

This implies a relative velocity between the bubbles and the water of the same magnitude as the maximum measured water velocities, and this violates a fundamental assumption of the heated plume analogy. The slip velocity reduces the effectiveness of the bubble as a buoyancy. The relative velocity between the bubbles and the rising water column gives rise to another difference from the heated plume. The bubble acts as a distributed smoothing screen and this may inhibit the development of large-scale eddies in the turbulent structure, and entrainment data derived from thermal plumes may not be appropriate.

These factors preclude a direct comparison with existing theories and make the extrapolation of the results beyond the range of the experiment uncertain. From the point of view of the oil well blowout the significant feature of these results is the self-containing effect of the surface flow. The following empirical relationship has been

developed for the dependence of the wave ring radius R metres, on gas flow rates and water depth.

$$R = 0.39z\left(\frac{V_f \times 10.36}{z + 10.36}\right)^{1/3}$$

where z is the water depth in metres and V_f if the volume flow of free gas m^3/min. This gives reasonable estimates within the range of test results but may not be applicable much beyond this range, i.e. water depths 33 m to 60 m and volume flows 3.6 to 40 m^3/min.

Figure 2.18(a) shows a view of the bubble plume operating in 60 m of water with 26.6 m^3/min of free air injected, the dark line beyond the instrument raft marks the wave ring. Figure 2.18(b) shows a real underwater blowout. The water depths are not known accurately but are probably less than 30 m. Comparing the centre of the surface boil with that of the 62 m^3/min flow obtained in the 23 m deep experiment suggests that the flow is considerably in excess of this value. The surface interaction region is distorted by a strong sea current, the 'arms' resulting from the shearing action between this and the flows induced by the plume. Similar distortions were seen during the experiment under strong wind conditions.

2.5 Conclusions

2.5.1 The rising gas bubbles entrain the surrounding water to form a rising plume which is initially conical in shape, but becomes cylindrical above a certain height. The plumes in 60 m of water became cylindrical about 23 m from the source. In shallow water of 23 m, the low flow plume, 3.6 m^3/min, remained conical throughout, with a divergence of 6° half angle, this angle increasing with increasing gas flow. It is thought that the height at which the plumes become cylindrical is determined by the local ratio of bubble volume to entrained water flow volume.

2.5.2 The mean centerline velocities did not vary significantly with either depth or air flow for a given plume height, being about 60 cm/sec for the 60 m plumes and 90 to 120 cm/sec for the 23 m plumes.

2.5.3 The interaction of the plume with the surface produces a ring of waves concentric with the plume centre which acts to confine surface debris. This wave ring marks a division in the direction of the radial surface flows, these being directed inwards at radii beyond the wave ring. In the case of an oil well blowout this feature should provide a certain amount of natural containment.

2.5.4 The behaviour of deep bubble plumes is not well described by present theoretical models and in the absence of such a model it is difficult to extrapolate the data far beyond the range covered by the present experiments. An appropriate theory is currently being developed by the present author.

2.6 References

Ashton G. D. Air bubble systems to suppress ice. Special Report 210, Cold Regions Research & Engineering Lab., U.S. Army, Hanover, New Hampshire. 1974.

Bulson, P. S. Currents produced by an air curtain in deep water. The Dock & Harbour Authority, Vol. 42, 1951, pp 15-22.

Carstens T. Prevention of ice formation by forced mixing. Proc. 1st Conf. in Port & Ocean Engineering under Arctic Conditions. Tech. Univ. Trondheim, Norway, August 1971, pp 140-151.

Datta, R. L., D. H. Napier and D. M. Newitt The properties and behaviour of gas bubbles formed at a circular orifice. Conf. on Formation & Properties of Gas Bubbles. Inst. of Chemical Engineers (London) Feb. 14, 1950.

Jones W. T. Air barriers as oil spill containment devices. J. Pet. Engr., April 1972, pp 126-142.

Kobus H. E. Analysis of the flow induced by air-bubble systems. Proc. 11th Conf. on Coastal Engineering, 1968, pp 1016-1031.

Topham D. R. Hydrodynamic aspects of an oil well blowout under sea ice. Interim Report, Beaufort Sea Project, Dec. 1974, Dept. of the Environment, Victoria, B.C.

Turner J. S. Buoyancy effects in fluids. Cambridge University Press, England, 1973, pp 195.

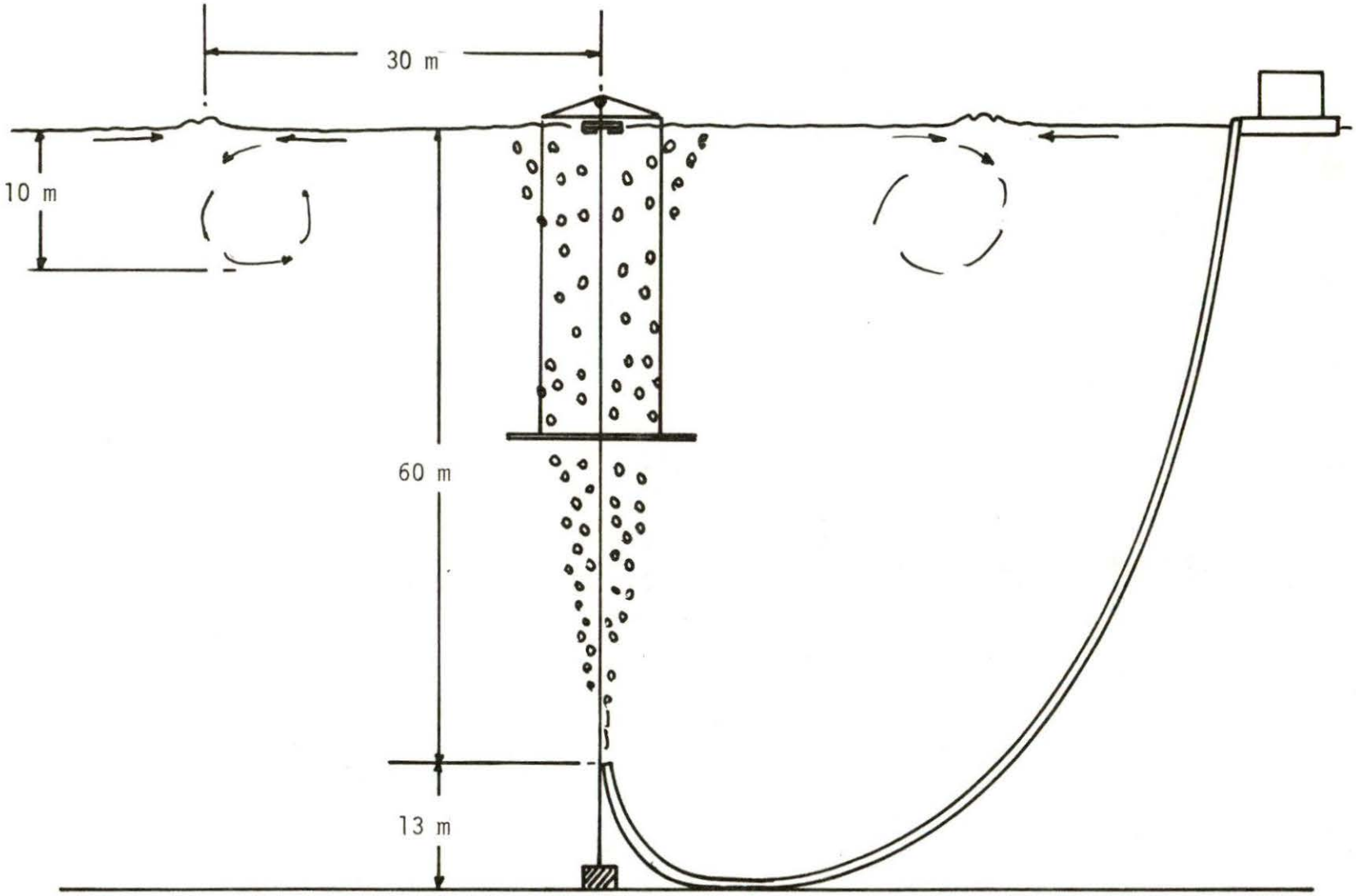

Fig. 2.1 Experimental Layout of Simulated Blowout

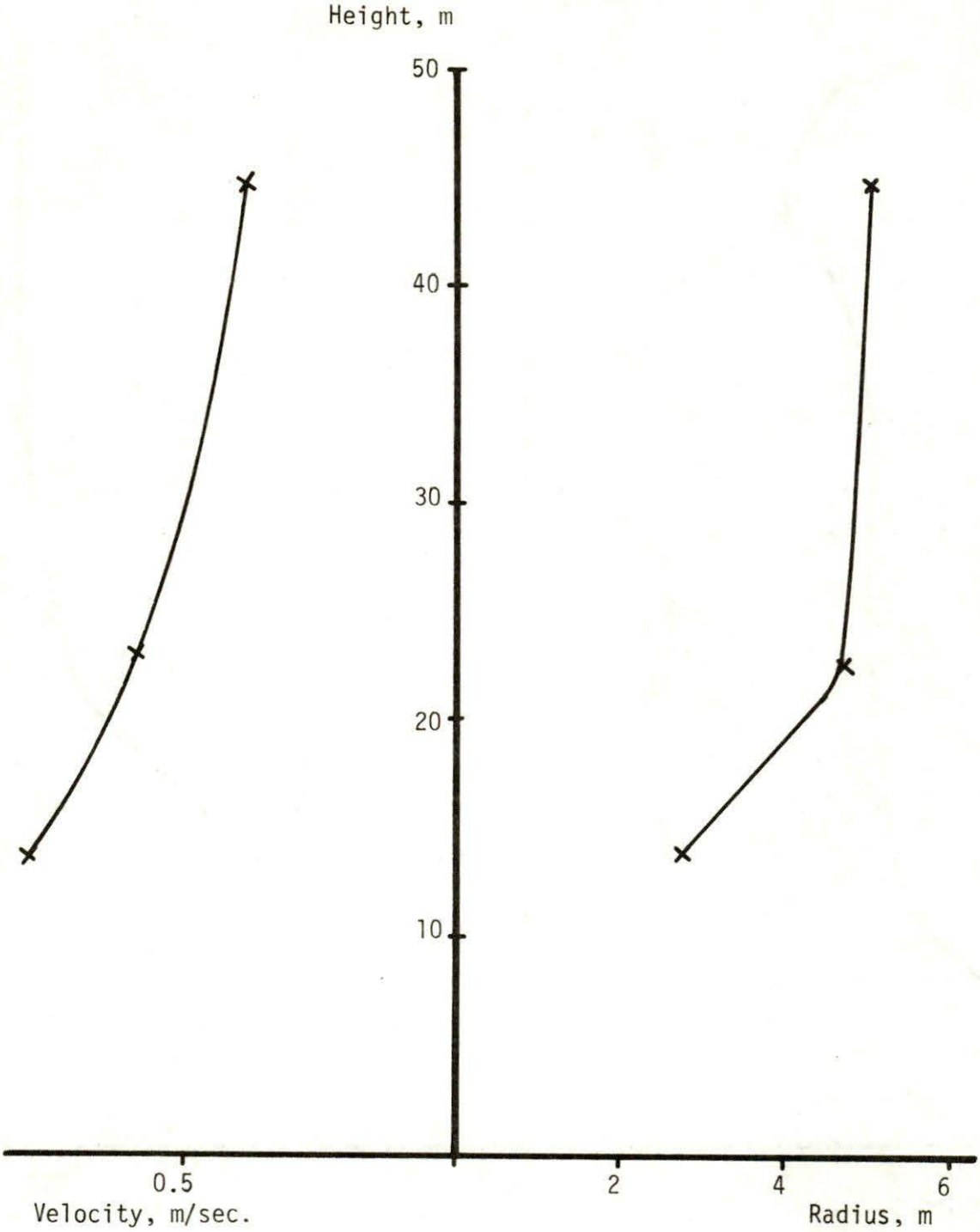

Fig. 2.2 Plume Shape, 11 m^3/min of free air at 60 m depth.

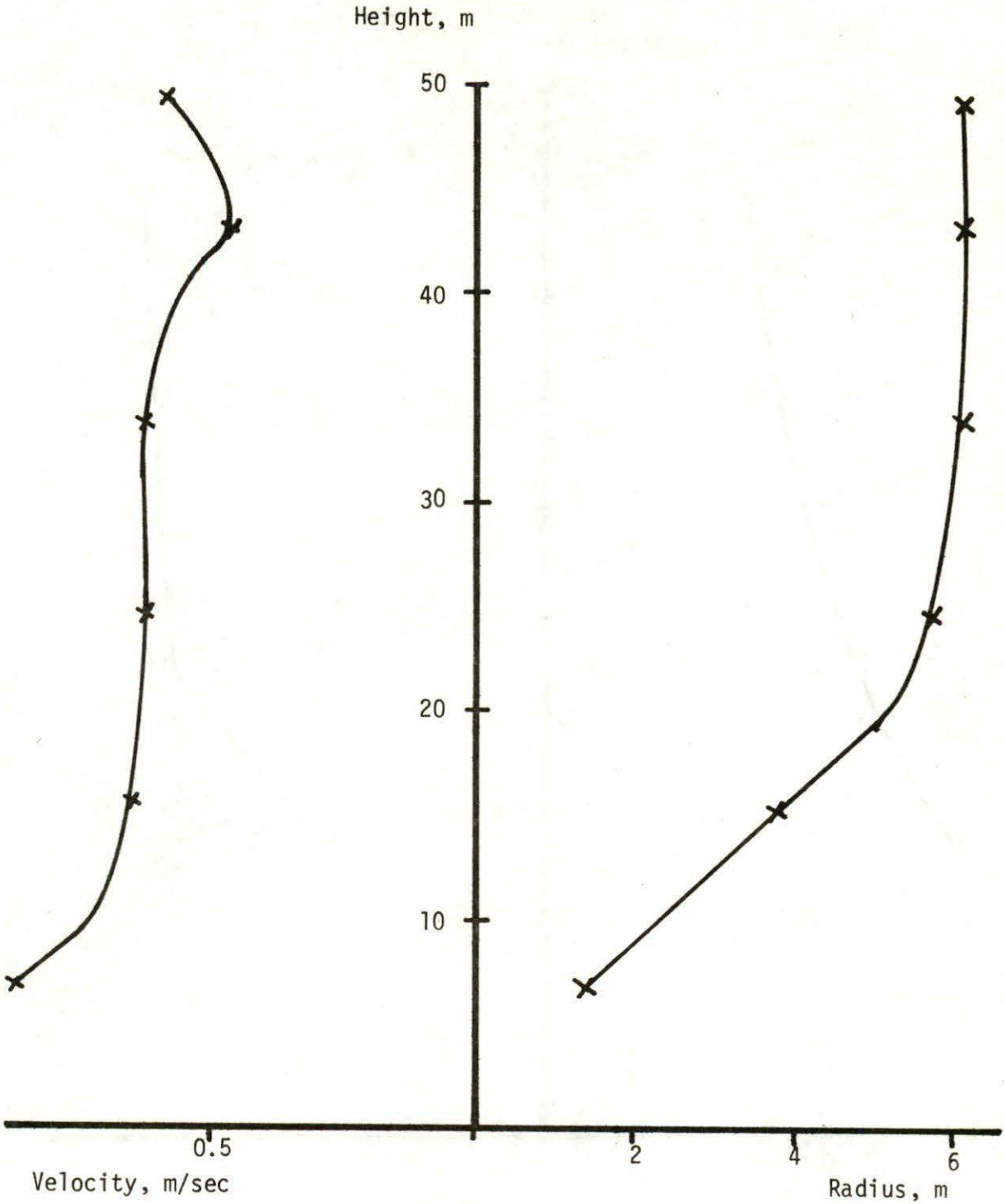

Fig. 2.3 Plume Shape, 22 m^3/min of free air at 60 m depth.

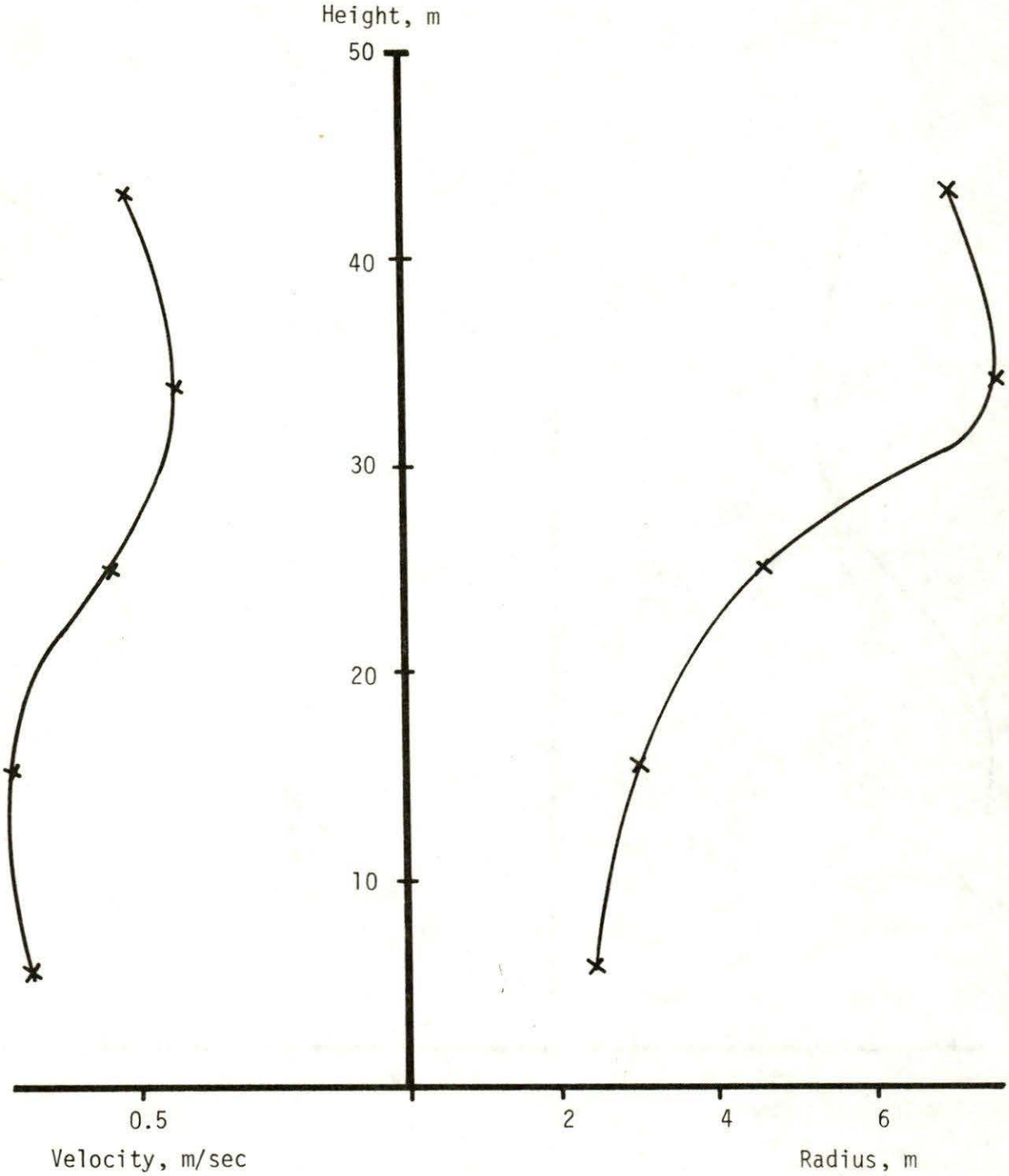

Fig. 2.4 Plume Shape, 26.6 m^3/min of free air at 60 m depth

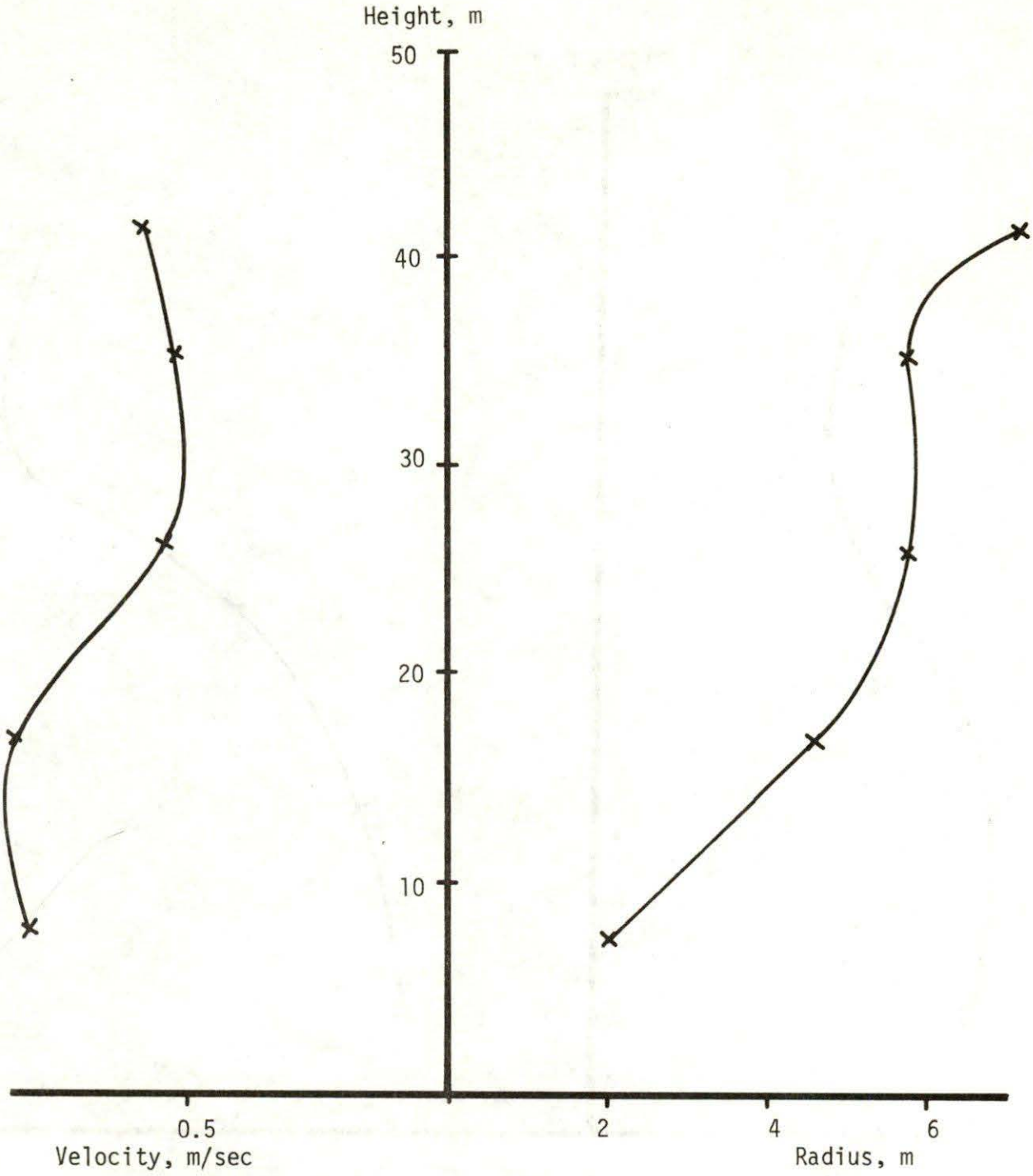

Fig. 2.5 Plume Shape 27.6 m^3/min of free air at 53 m depth.

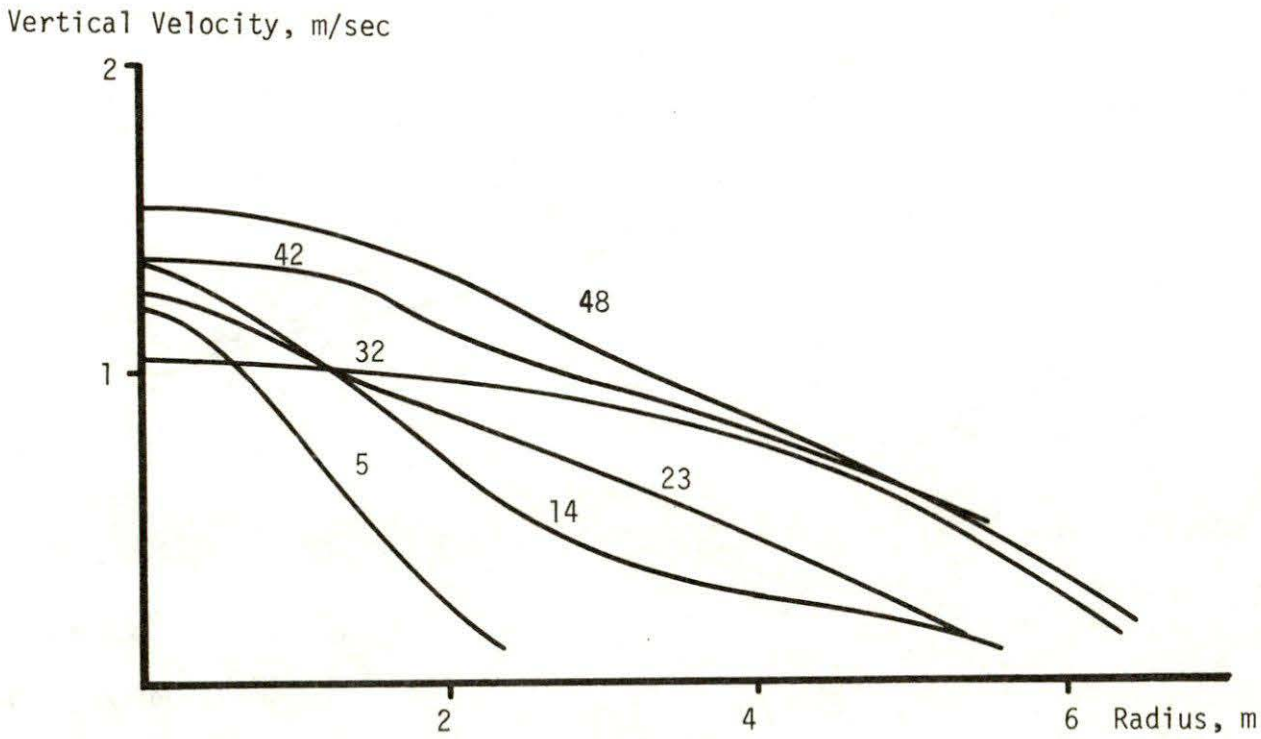

Fig. 2.6 Velocity Profiles for 22 m^3/min of free air at 60 m depth
Numbers on curves indicate depth in metres.

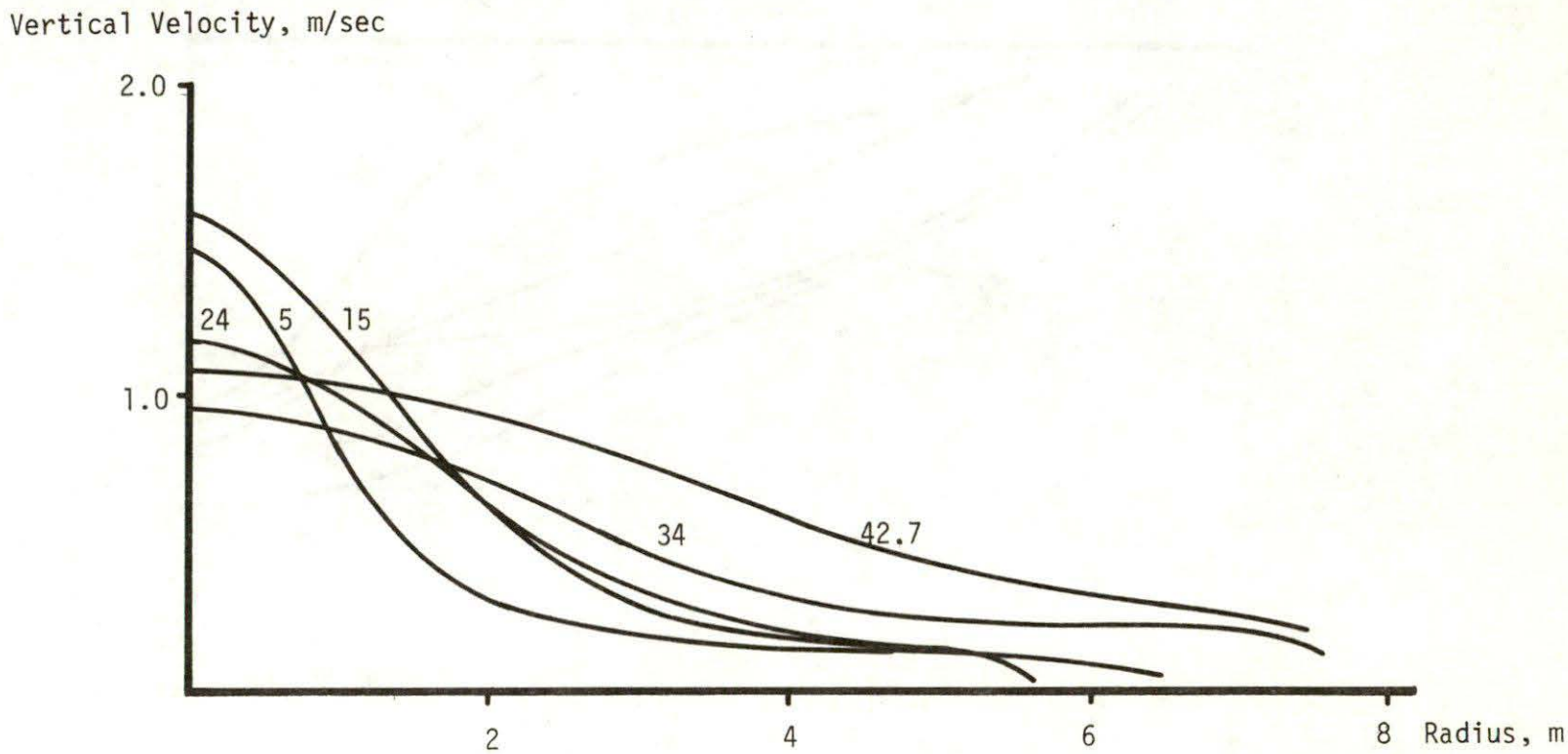

Fig. 2.7 Velocity Profiles for 26.6 m^3/sec of free air at 60 m depth, Numbers on curves indicate depth in metres.

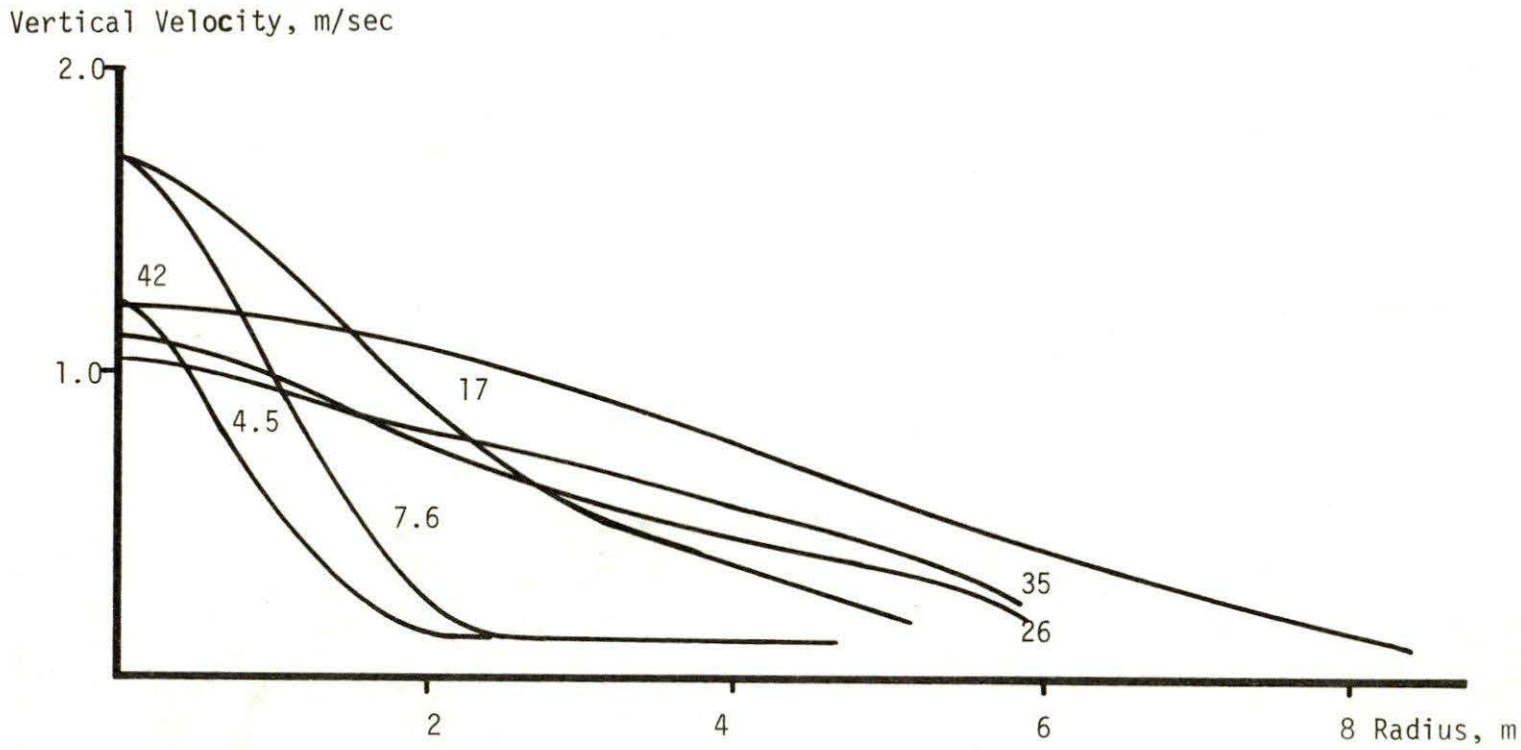

Fig. 2.8 Velocity Profiles for 27.6 m^3/sec of free air at 53 m depth. Numbers on curves indicate depth in metres.

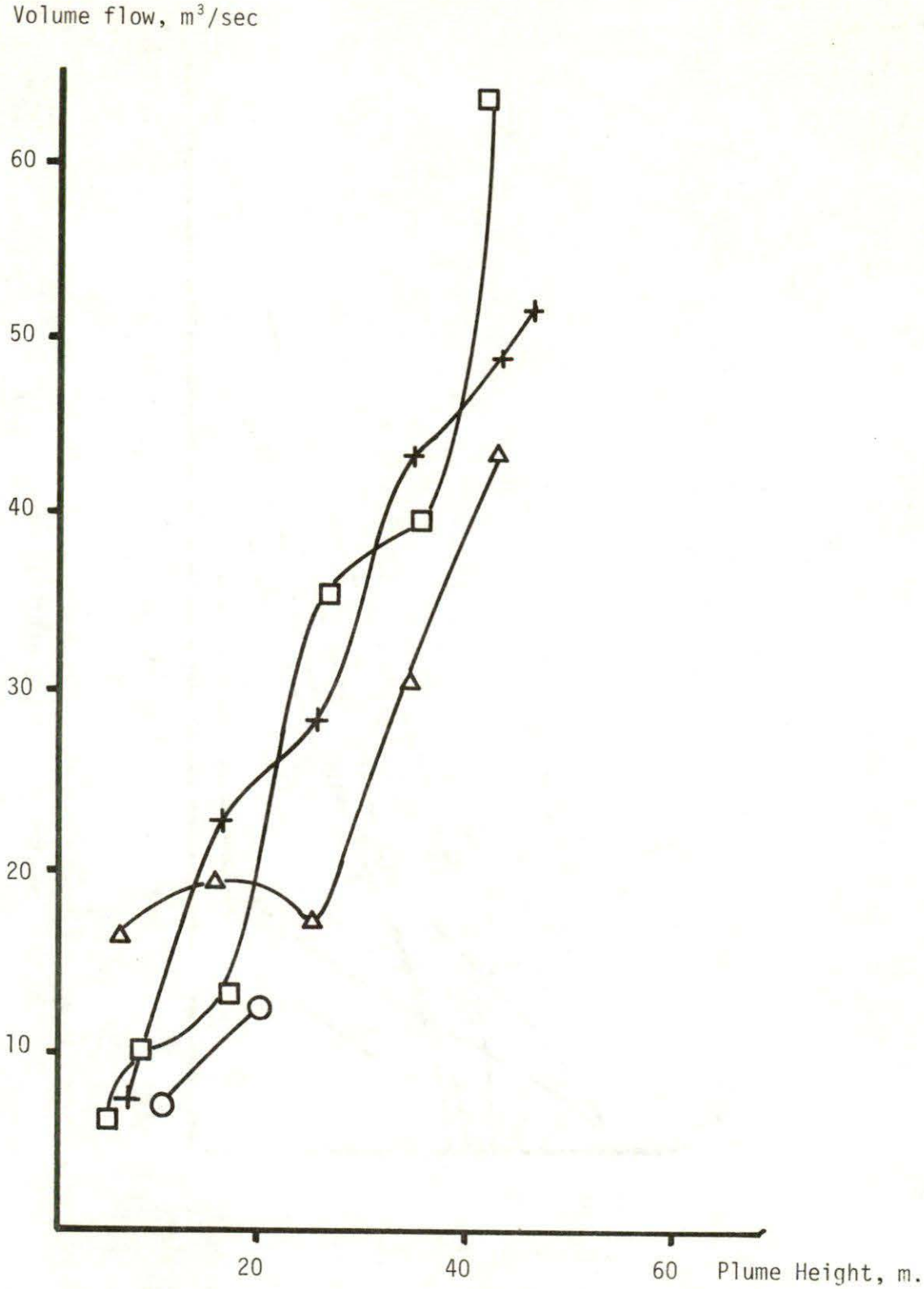

Fig. 2.9 Variation of total vertical volume flow of water with height, O.11 m^3/min, +.22 m^3/min, Δ26.6 m^3/min, □27.6 m^3/min of free air.

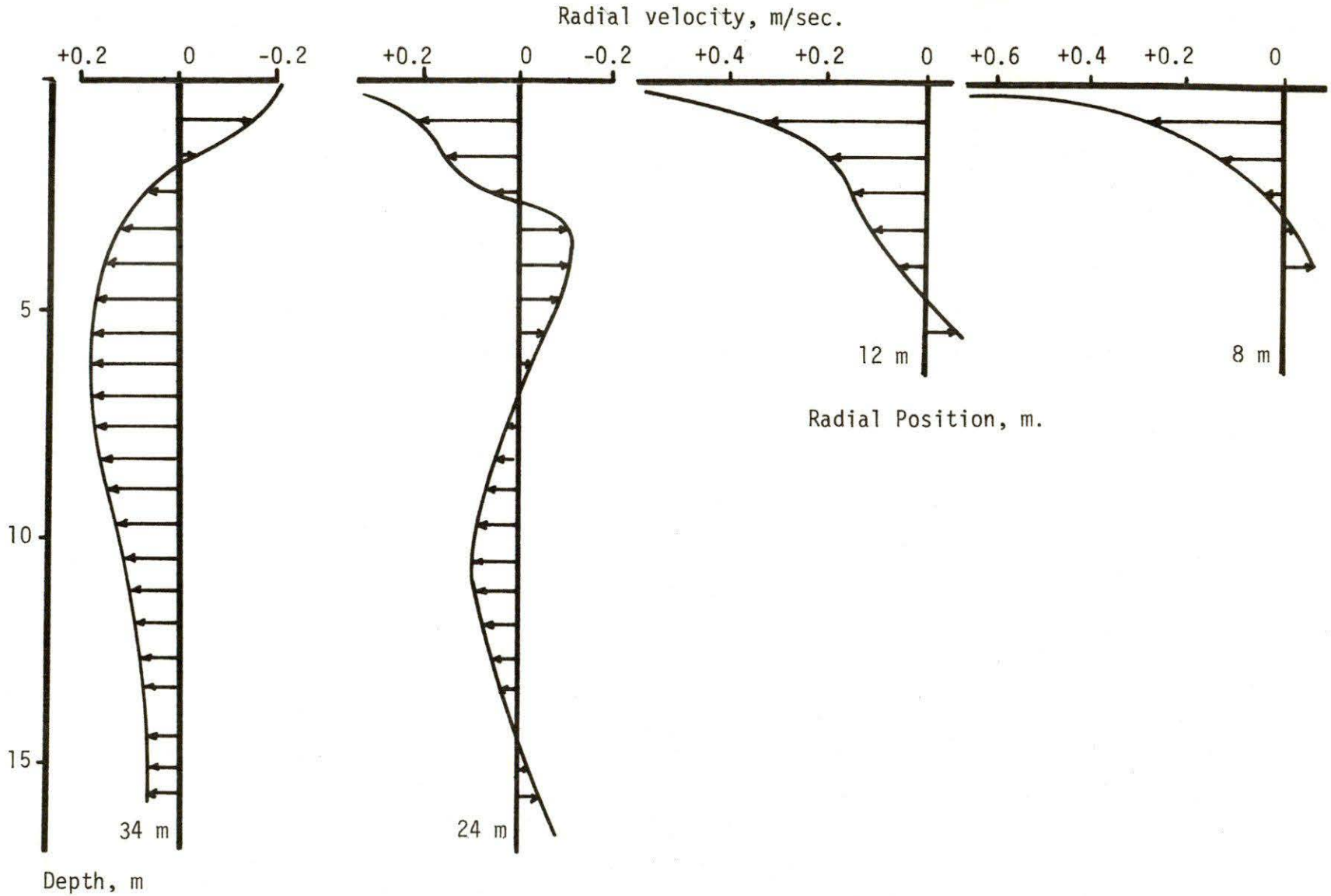

Fig. 2.10 Radial Velocity Profiles of Induced Currents, 26.6 m^3/sec air at 60 m depth.

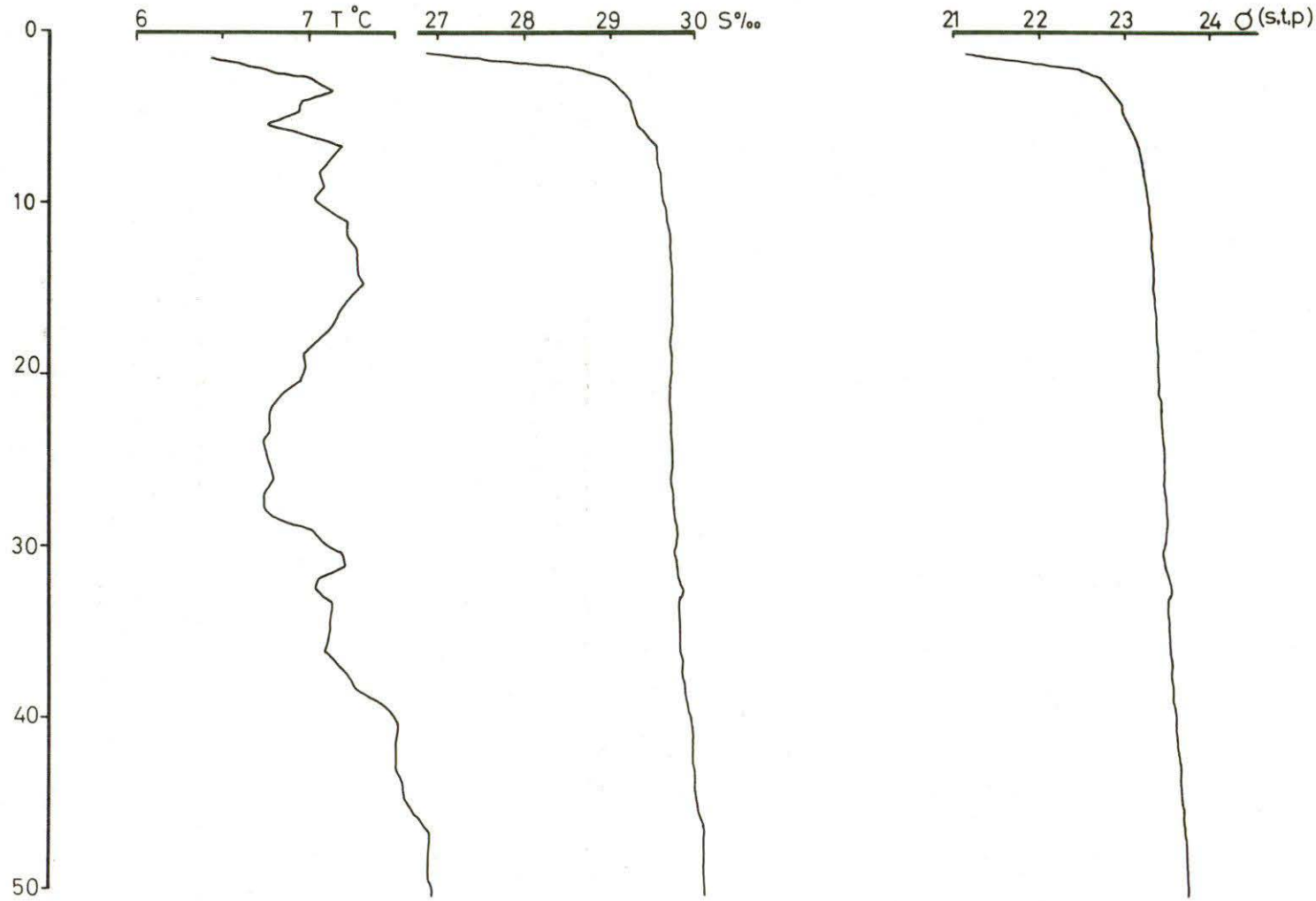

Fig. 2.11 Temperature, salinity and density profiles, 60 m site, without plume.

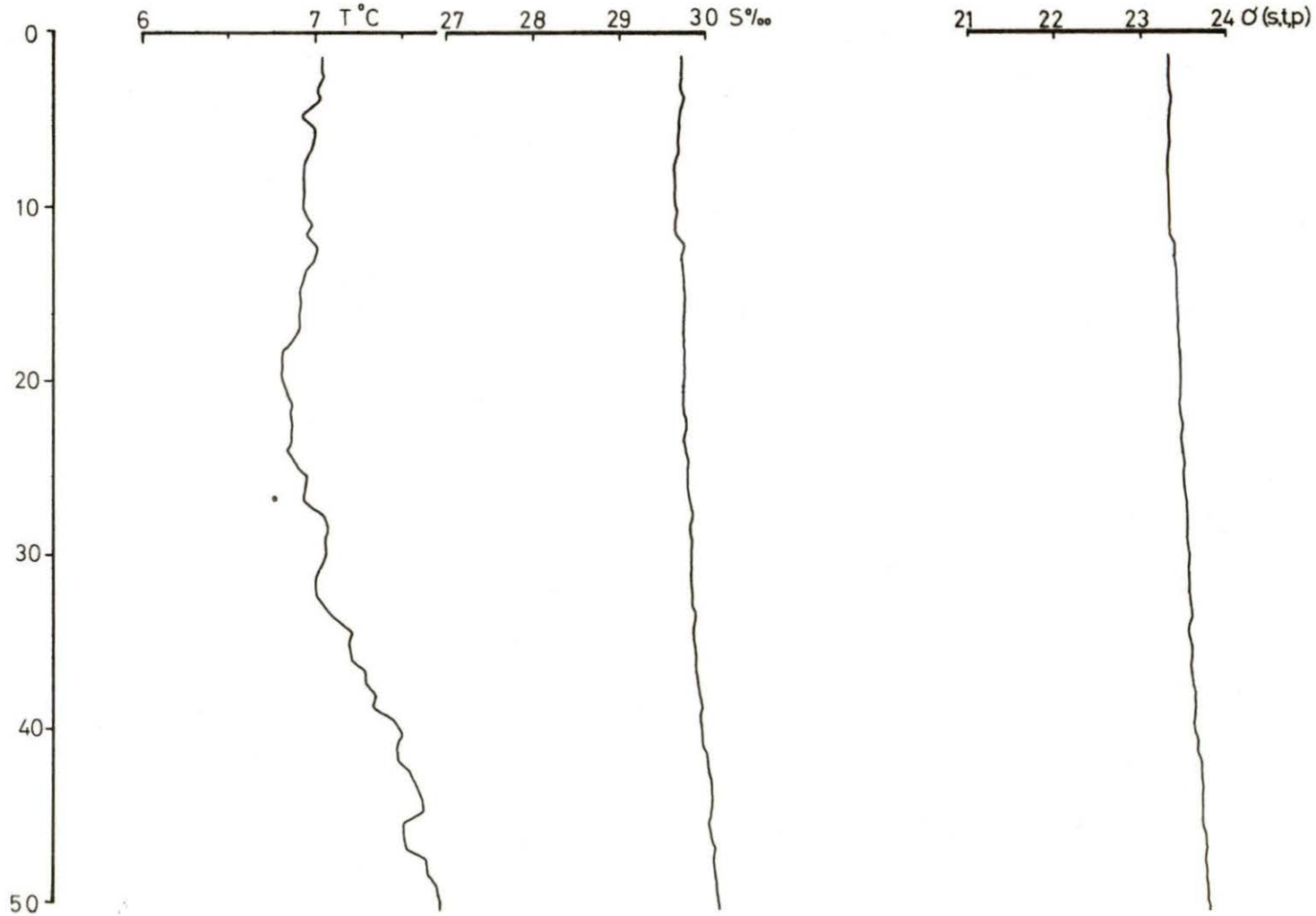

Fig. 2.12 Temperature, salinity and density profiles, 60 m site, with plumes.

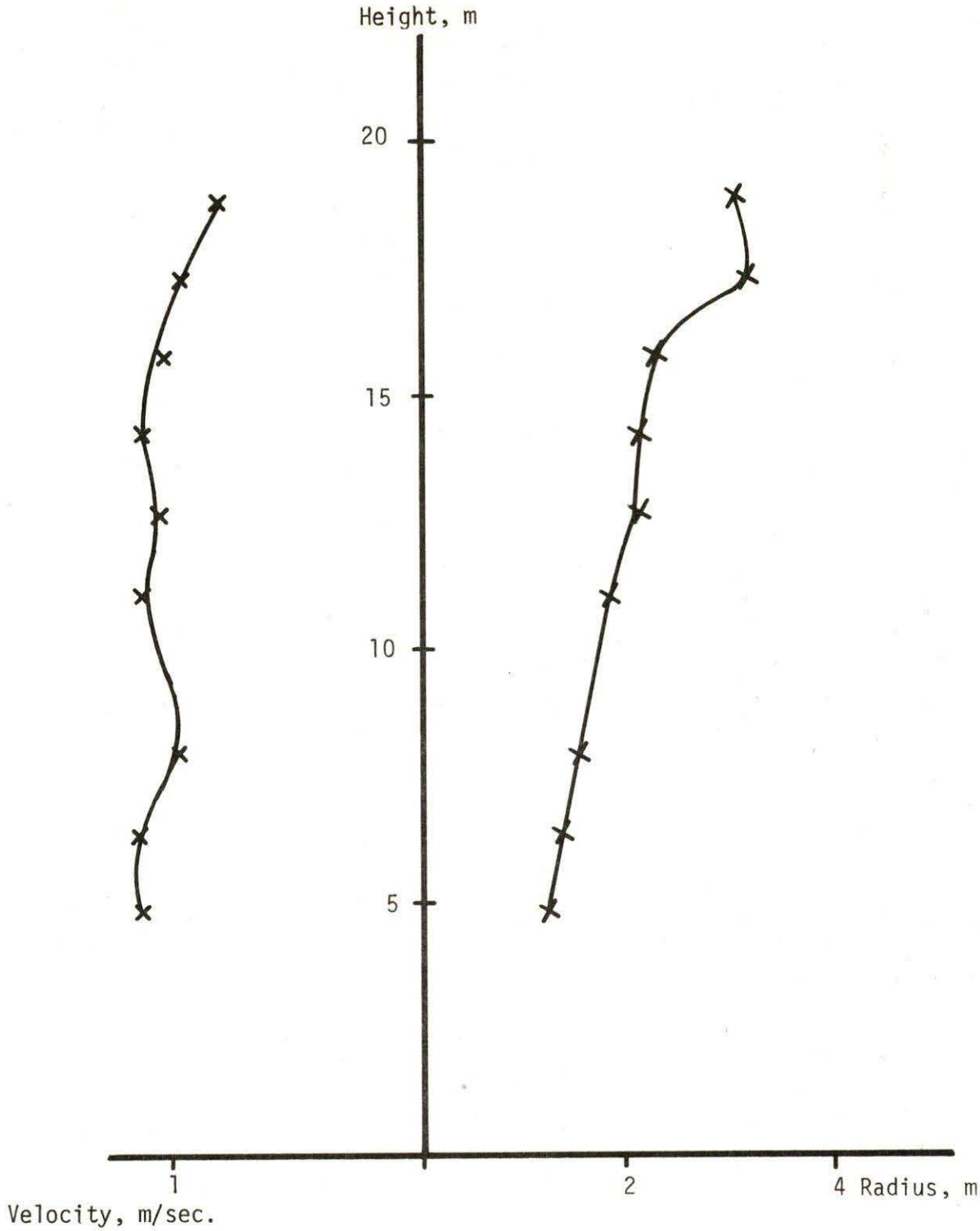

Fig. 2.13 Plume Shape, 3.6 m^3/min of free air at 23 m depth.

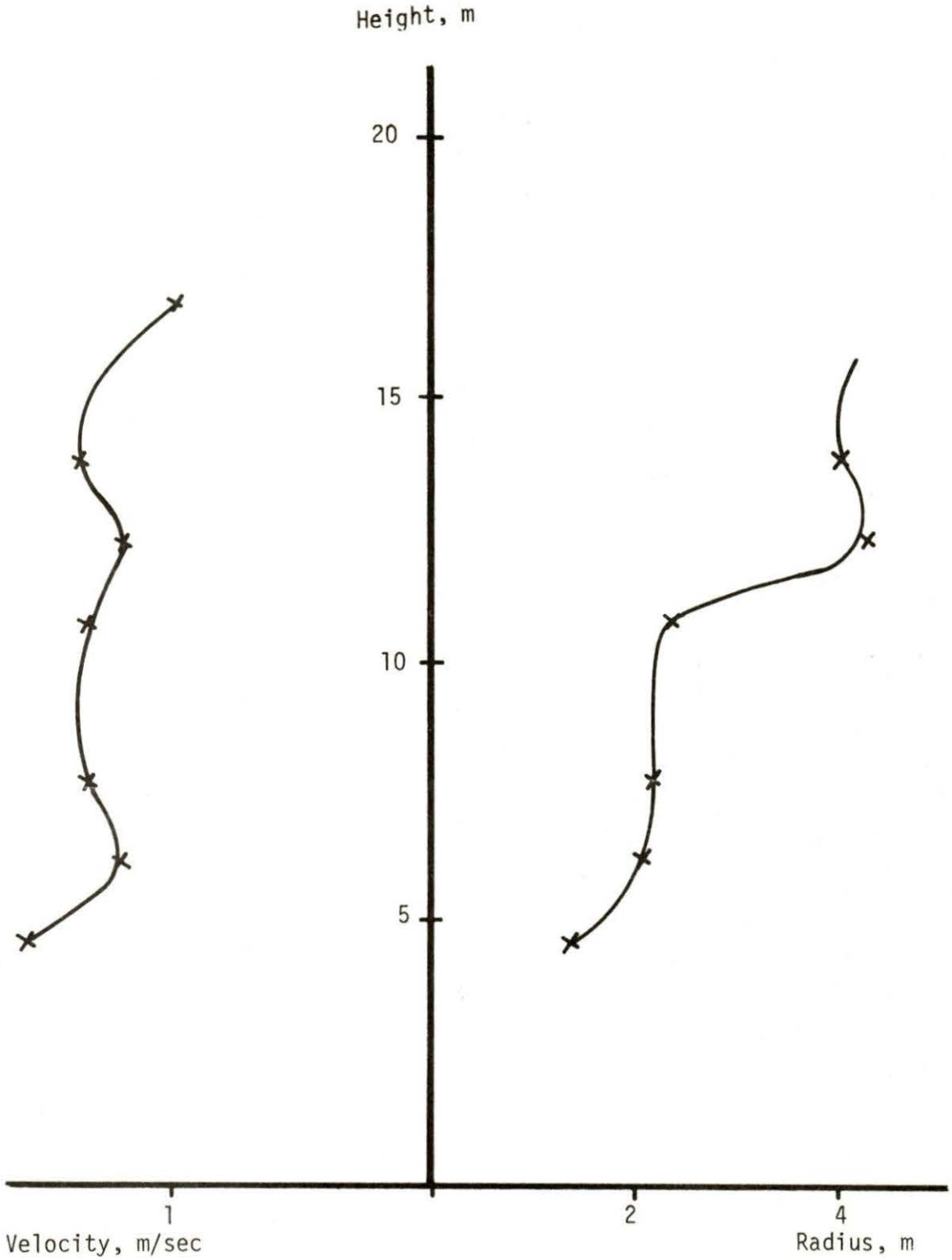

Fig. 2.14 Plume Shape, 29 m^3/min of free air at 23 m depth

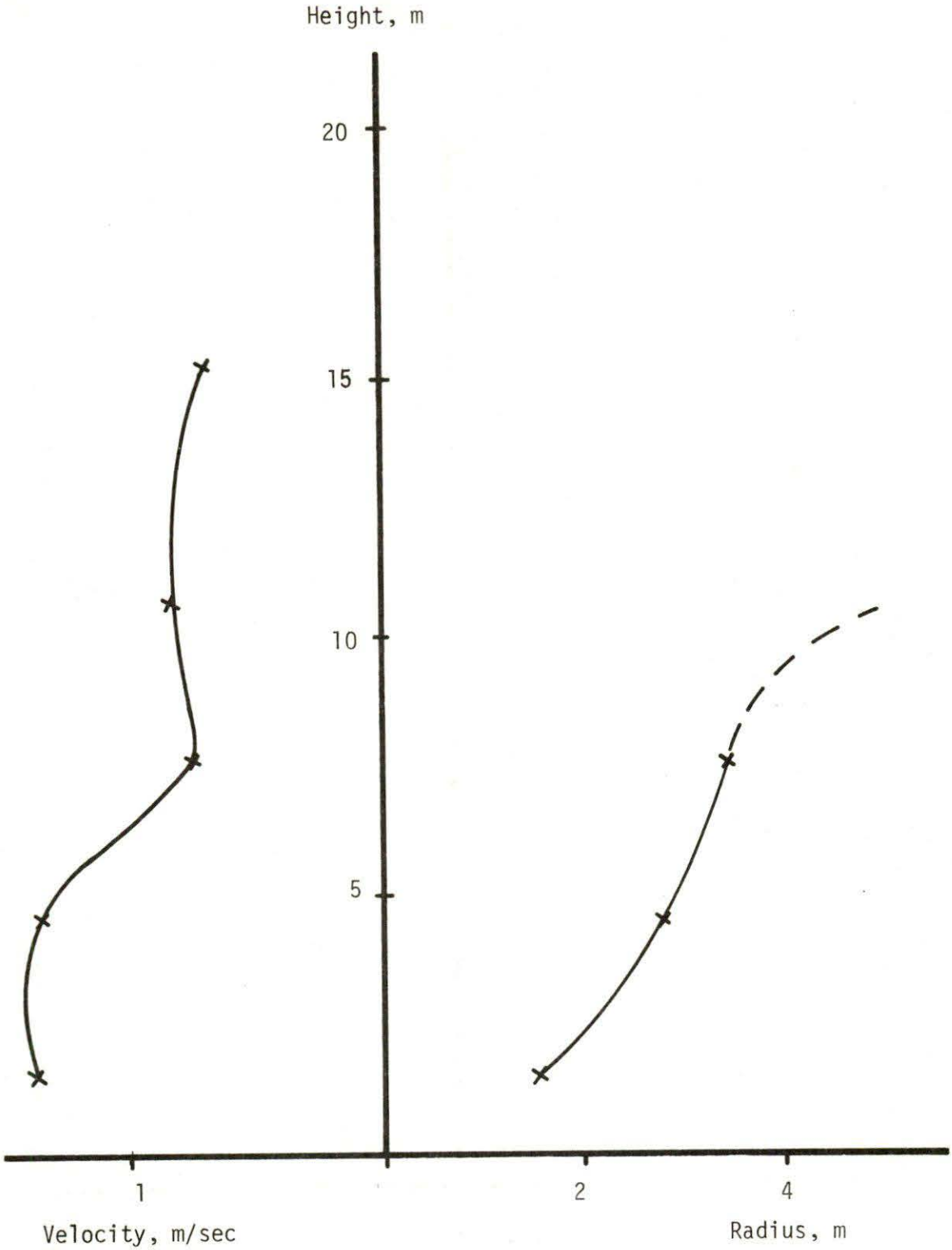

Fig. 2.15 Plume Shape, 40 m^3/min of free air at 23 m depth.

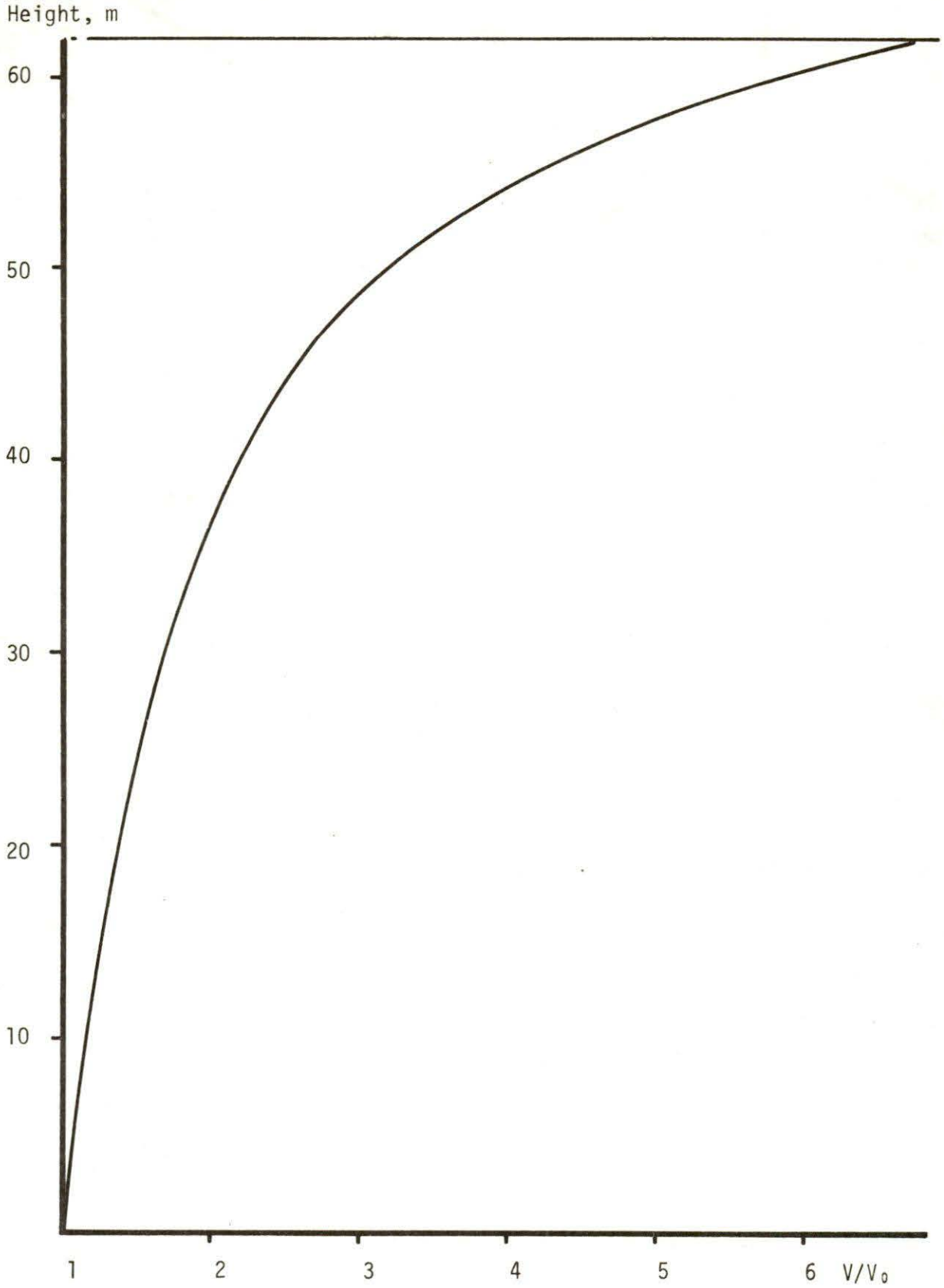

Fig. 2.16 Change of Relative Buoyancy with Height, 16 m.

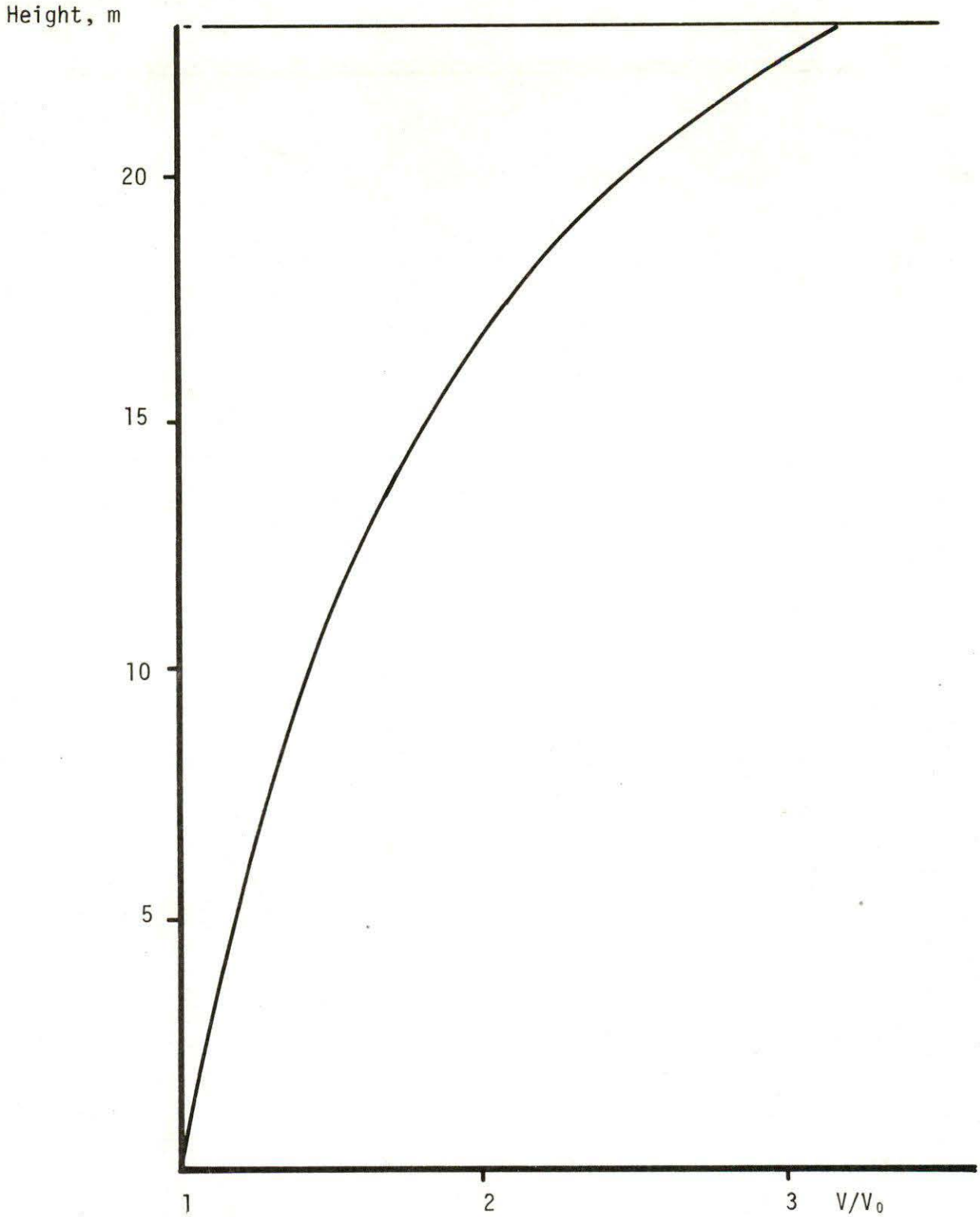

Fig. 2.17 Change of Relative Buoyancy with Height, 23 m.

(a)

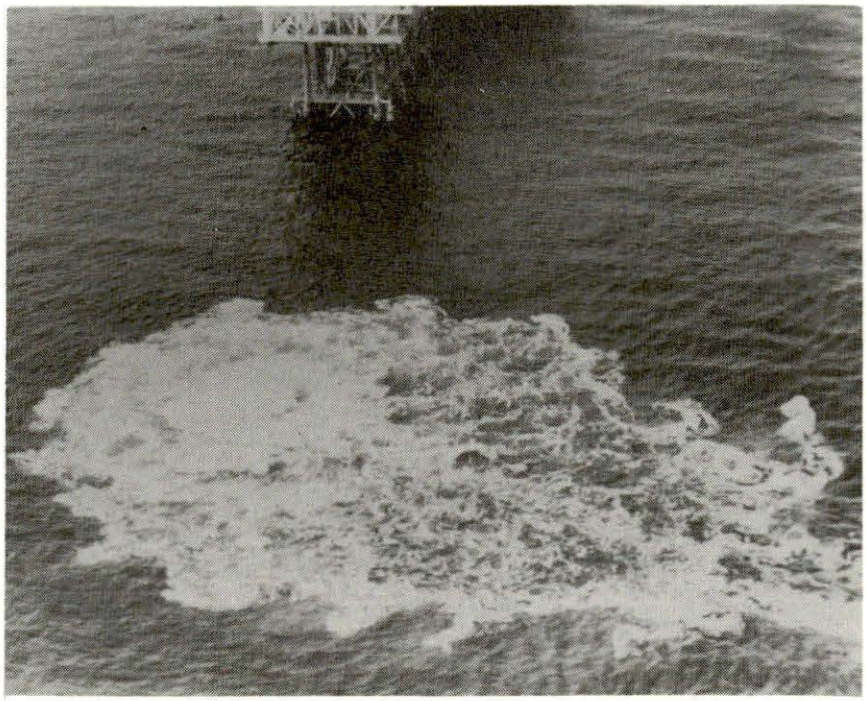

(b)

Fig. 2.18 (a) simulated blowout, (b) underwater gas flare

3. THE BEHAVIOUR OF CRUDE OIL/GAS MIXTURES INJECTED UNDER WATER

3.1 Introduction

The work in this section was carried out to examine the possibility of stable emulsions being formed close to the well exit, in particular any occurrence of the water-in-oil emulsions encountered in some open sea oil spills - 'chocolate mousse' formations. These are known to be very stable and as their specific gravity is close to that of water they are easily transported by sea currents.

The test conditions selected again correspond to those of the 'standard Beaufort Sea Project oil well', i.e. initial flow rates of 2500 barrels/day (398 m^3/day), with a gas content of 22.7 m^3 of free gas/barrel with a range of seawater depths detween 15 m and 180 m. A pipe diameter of 15 cm was taken as the well exit condition. Calculations on the basis of this orifice immersed in 15 m and 180 m of seawater with the above gas and oil flows yield the following flow velocities.

TABLE 1

Depth m	Superficial gas velocity m/sec	Superficial oil velocity m/sec
15	14.3	0.25
180	1.92	0.25

The superficial velocity being that which each fluid would have if occupying the pipe alone.

Two types of crude oil were selected for testing, Norman Wells crude oil supplied by Imperial Oil Limited and Swan Hills crude oil supplied by Gulf Oil Limited. The physical properties of the two oils at 25°C are shown below.

TABLE 2

Oil Type	Specific Gravity	Viscosity	Pour Point	Surface Tension
Norman Wells	0.821	6.0 c.p.	-50°C	24.7 dyns/cm
Swan Hills	0.815	6.5 c.p.		26.3 dyns/cm

These oils are considered to represent extremes of those types expected to be found in the Beaufort Sea and are those used in related studies of the effects of oil in sea ice (NORCOR 1975).

3.2 Test Techniques

It was anticipated that any mechanism forming an emulsion close to the nozzle would be complex in nature and that it was unlikely that

simple scaling parameters could be devised for model testing. Tests were therefore carried out under conditions as closely approaching full scale as was practical under the time scale of the study. By testing a number of different scale systems the important parameters controlling the processes could be identified.

Tests were conducted in an oval cross section tank of 68 litres capacity (standard domestic oil storage tank) containing approximately 1.5 m depth of water, Fig. 3.1. Oil and gas were injected separately into a 2.2 cm diameter mixing chamber beneath the tank and fed into the water through a vertical feed pipe. Feed pipe diameters of 0.64, 2.2, 7.6 and 14.7 cm were used to change the scale of the experiment. The length of the feed pipe was 70 cm for the 0.64 cm and 2.2 cm diameter pipe, giving in excess of 20 pipe diameters for the oil/gas mixtures to stablize. Lengths of 90 cm were used for the 7.6 and 14.7 cm diameter pipes, this being the longest length that could be accommodated and still leave an adequate water depth to the surface.

Flow durations of the order of 3 to 5 seconds were sufficient to establish stabilized flow patterns and tests were carried out in both sea water and fresh water with gas only injected and with gas/oil mixtures. Nitrogen was used as a test gas rather than methane to reduce explosion hazard, the main difference between the two being the greater solubility of methane in water, and close to the nozzle the time scale is too short for this to be significant. It was also assumed that the oil/gas mixture leaving the well exit would be in equilibrium and that gas did not rapidly come out of solution in the oil as it left the nozzle.

Both still and cine films of the resulting bubble systems were taken through windows covering the full depth of the tank. In addition microscopic photography was employed to obtain an estimate of the small scale droplet distributions remaining suspended in the tank after firing.

The configuration of the oil/gas mixture within the exit pipe was felt to be of some importance and this is known to be a strong function of the superficial oil and gas velocities in the pipe (Govier and Aziz 1972). The flow conditions given in Table 1 result in different flow regimes for the two extremes of water depth. In the 180 m case the flow is expected to be of the 'slug' type with alternate sections of oil and gas emerging. For the flow conditions corresponding to 15 m of water the flow is expected to be of an annular pattern with the oil flowing up the sides of the pipe and the gas up the centre. The flow volumes of gas and oil were therefore adjusted to give the same superficial velocities for each pipe size corresponding to those of Table 1.

The gas flow rates were calibrated by inverting a water filled container over the pipe exit and measuring the volume of water displaced over a known flow period. This gave flow calibrations to an accuracy of ±10%. Oil flows were obtained directly from measurements of the injected volumes.

3.3 Results

The results were all obtained in the form of either single flash pictures, exposure approximately 1/1000 sec or cine film taken at 64 frames/sec with an exposure of approximately 1/200 sec. For each set of test conditions photographs were taken showing gas alone being injected and gas with the appropriate addition of oil. For the tests with oil injection an attempt was made to determine droplet size distributions from the photographs. These had to be confined to the edges of the plumes where individual droplets could be clearly distinguished and were limited by the resolution to droplets of approximately 0.5 mm diameter. For one set of conditions the small drops left suspended after a test firing were photographed through a microscope focussed into the interior of the tank. Knowing the magnification and depth of field the droplet density distribution was estimated. extending the resolution down to 15 microns (1 micron = 10^{-6}m).

The behaviour of gas bubbles formed at submerged orifices has been extensively studied and is well understood for low flow rates and small orifices where surface tension and buoyancy are the dominating forces. Single bubbles form and are released when the buoyancy force becomes equal to the holding force of the surface tension around the pipe exit. The ratio of bubble radius to pipe exit radius at the moment of release becomes

$$\frac{R}{r} = \left(\frac{3}{2}\,\frac{\sigma}{r^2\rho g}\right)^{1/3}$$

where R is the bubble radius at release and r the pipe radius, thus it can be seen that bubble size does not scale geometrically with pipe radius.

As gas flow rates are increased the dynamic pressure forces arising from the rapid bubble expansion come into play and considerably modify the expanding bubble shape. In addition, the bubbles merge into each other at the pipe exit. As the size of the orifice is increased the emergent bubbles fracture into small bubbles within a short distance. The overall picture of bubble behaviour over the range of nozzle sizes and gas flow rates tested is one of rounded bubbles growing from the orifice, releasing and bursting into smaller fragments. At the higher flow velocity the emerging bubbles have a fluted surface appearance and the bursting is more violent. As the nozzle exit is increased in diameter the bubbles became flattened horizontally and the breakaway is again accompanied by more violent bursting.

Typical bubble configurations for the pipe sizes tested are sketched in Figures 3.2, 3.3, 3.4 and 3.5. The apparatus was too small in scale to allow testing the 7.6 cm and 14.7 cm diameter pipes at 14 m/sec gas exit velocity.

With simultaneous injection of oil and gas the oil appears to be drawn around the surface of the emerging bubble and shattered into small droplets during the release and breakup of the bubble. These droplets are then carried upwards with the rising bubble column. Figure 3.6 shows still photographs of nitrogen being injected under water through the 2.2 cm diameter pipe at exit velocities of 1.9 m/sec and 14 m/sec, and Figure 3.7 the same gas flow conditions with the addition of Norman Wells crude oil to the flow.

Photographs of the gas and oil column were analyzed for droplet size distribution for the following cases:

TABLE 3

Pipe dia.	Water Type	Gas Exit Vel.	Oil Type
0.64 cm	fresh	1.9 m/sec	Norman Wells
"	"	14 m/sec	" "
2.2 cm	"	1.9 m/sec	" "
"	"	14 m/sec	" "
"	sea	1.9 m/sec	" "
"	"	14 m/sec	" "
"	fresh	1.9 m/sec	Swan Hills

Graphs of the resulting droplet distributions are shown in Figures 3.8, 3.9, 3.10 and 3.11. As noted earlier these distributions are confined to the edges of the plumes and limited in resolution to 0.5 mm. Each sample consisted of a count of approximately 100 drops total. This sample size is rather small and the graphs should be regarded as indications of drop sizes rather than definitive distribution functions. The results reflect the bubble behaviour in that the most marked differences can be seen between the 1.9 m/sec and 14 m/sec gas velocity exit conditions with a concentration towards the smaller sizes for the 14 m/sec gas flow velocity.

The apparatus was not capable of delivering sufficient oil volume flows to the 7.6 and 14.7 cm diameter pipes, and in these cases most of the droplets seemed to be 0.5 mm or less in diameter. The violent mixing caused by these large jets rapidly distributed the droplets over the tank volume, considerably reducing the clarity of the photographs to a point where droplet distribution functions could not be obtained.

Microscopic photography was employed to obtain the density distribution of small size droplets for the case of Swan Hills crude injected into fresh water through the 2.2 cm diameter pipe with 1.9 m/sec gas exit velocity. These show a strong peak at about

15 microns diameter. The microscope was focussed into the interior of the tank through an air filled extension tube fixed to the inside of the window. The oil/gas mixture was injected and left to stand for five minutes. This allowed the circulation patterns set up by the jet to distribute small droplets throughout the tank and also for large scale droplets to rise to the surface, the droplet sizes of interest being those which would easily be carried with water movement if they escaped from the rising bubble column. Photographs were taken at random intervals with different magnifications, and knowing the depth of focus, an approximate density distribution was calculated (Figure 3.12). The total sample consisted of a count of 140 droplets. To check that the droplets were formed at the pipe exit and not by the bubbles hitting a layer of oil at the surface of the water, separate tests were made firing gas only with oil floating on the water. Drops of the order of 2-3 mm were formed with no sign of microscopic particles.

The density distribution of Figure 3.12 was obtained at half the tank depth and assuming that this is uniform over the tank volume, a figure of 1% is obtained for the proportion of injected oil suspended in a fine enough form to be easily carried by water movements.

3.4 Discussion

One of the motivations for this experiment was the question of whether or not stable emulsions could be formed close to the sea bed. The violent bursting action of the oil covered gas bubbles at the pipe exit produces a finely divided suspension of oil droplets in water, and the nature of this splitting process is such that a continuous volume of water-in-oil emulsion is unlikely to be formed even with oil containing surfactants favouring such formations.

The water volume flows entrained by the rising gas bubbles are such that the average density of 1 mm diameter oil droplets in the water column is 1 per cm^3, and coalescence during their rise is unlikely. The remaining question to be answered is the behaviour of the oil on reaching the surface. According to Canevari, 1969, most naturally occuring oils favour the formation of water-in-oil emulsions and an initial dispersion of oil drops of this type in water reverts to a continuous oil slick at the surface. It is only by the addition of further mixing energy to this continuous slick that water-in-oil emulsion is formed. Thus oil droplets rising under an ice sheet would quickly collect into a pool.

At a late stage in the investigation it came to light that a sample of Swan Hills crude used in related tests on sessile drop behaviour, Rosseneger 1975, formed under certain mixing conditions, much more stable water-in-oil emulsions than the sample used in the injection tests. Supplementary tests were therefore carried out to compare the behaviour of these two samples, henceforth referred to as samples I and II respectively. Two tests were performed. In the first, air was bubbled continuously for several hours through a layer of oil floating on water. Sample I rapidly formed a water-in-oil emulsion,

a large proportion of which remained stable for many days at room temperature. With Sample II, although water-in-oil emulsion was formed, a large proportion reverted to a continuous oil slick within minutes of the cessation of bubbling.

In the second test oil was injected into water through a fine syringe to produce a suspension of droplets which was allowed to coalesce at the surface to simulate the final stages of the rise of the oil droplets produced in the blowout. Under these conditions both samples coalesced into continuous slicks. The problem of the formation of stable emulsions is thus one of surface mixing and in this respect reduces to the case of an open water oil spill.

3.5 Conclusions

3.5.1 Tests were performed injecting both Norman Wells and Swan Hills crude oil concurrently with nitrogen gas at velocities of 1.9 and 14 m/sec into both sea water and fresh water to simulate an undersea oil well blowout. Pipe exit diameters of 0.64, 2.2, 7.6 and 14.7 cm were used. The release of the bubbles at the pipe exit breaks the oil into fine droplets. In general the higher flow velocity produced smaller droplet sizes, as did the larger pipe diameters, this being associated with greater violence in the bubble release. The major portion of the oil was contained in droplets in the range 0.5 to 1.0 mm diameter. These have terminal velocities between 5 and 7 cm/sec and if they escape from the main plume of bubbles and entrained water, will rise to the surface in a comparatively short space of time.

3.5.2 A small proportion, of the order of 1%, of the oil injected, is in drops of less than 50 microns diamater whose terminal rise velocity is 0.5 mm/sec or less and these could be mixed downwards to depths of 10 m at the outer edges of the plume/surface interaction region, and from there be carried away by small ocean currents.

3.6 References

Govier, G.W. and K.Aziz. The flow of complex mixtures in pipes. Van Norstrand Reinhold Co. 1972.

Dickens, D, J. Overall and R. Brown, NORCOR Engineering The interaction of crude oil with Arctic sea ice. DSS Contract number OSV4-0043. September 1975.

Rosenegger L. W. Movement of oil under sea ice. Imperial Oil Ltd. Production Dept. Lab., Calgary, Alberta, October 1975

Canevari G. P. General dispersant theory. Proc. of Joint Conf. on Prevention & Control of Oil Spills, Amer. Pet. Inst., Dec. 15-17, 1969, Americana Hotel, New York

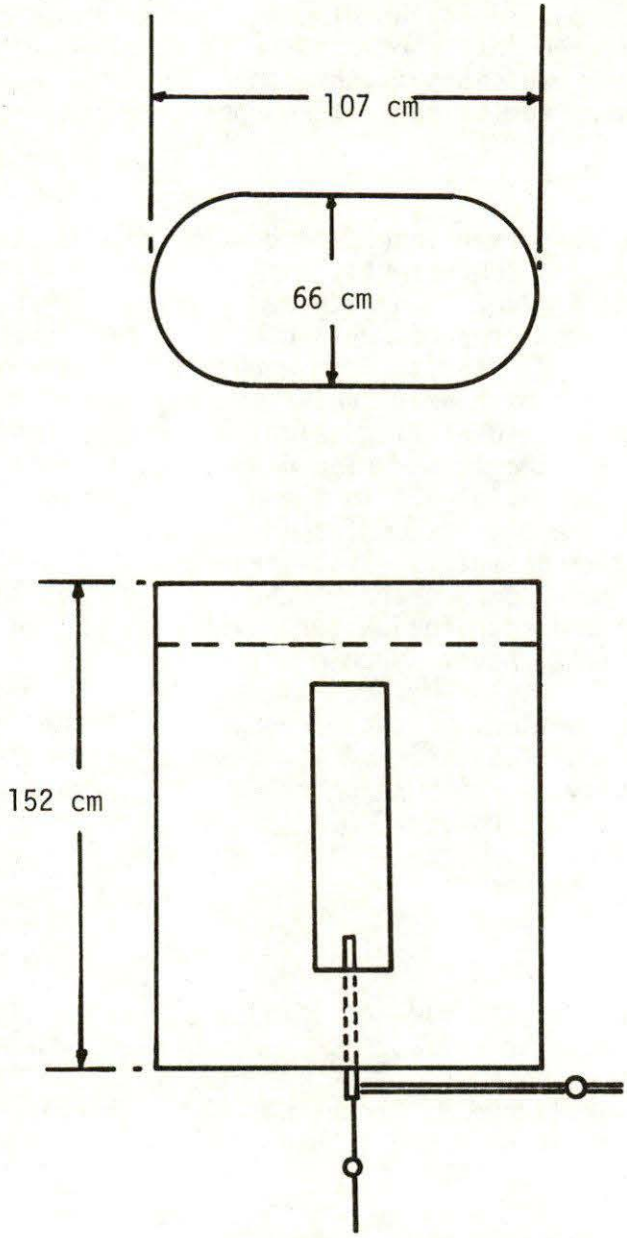

Fig. 3.1 Experimental apparatus.

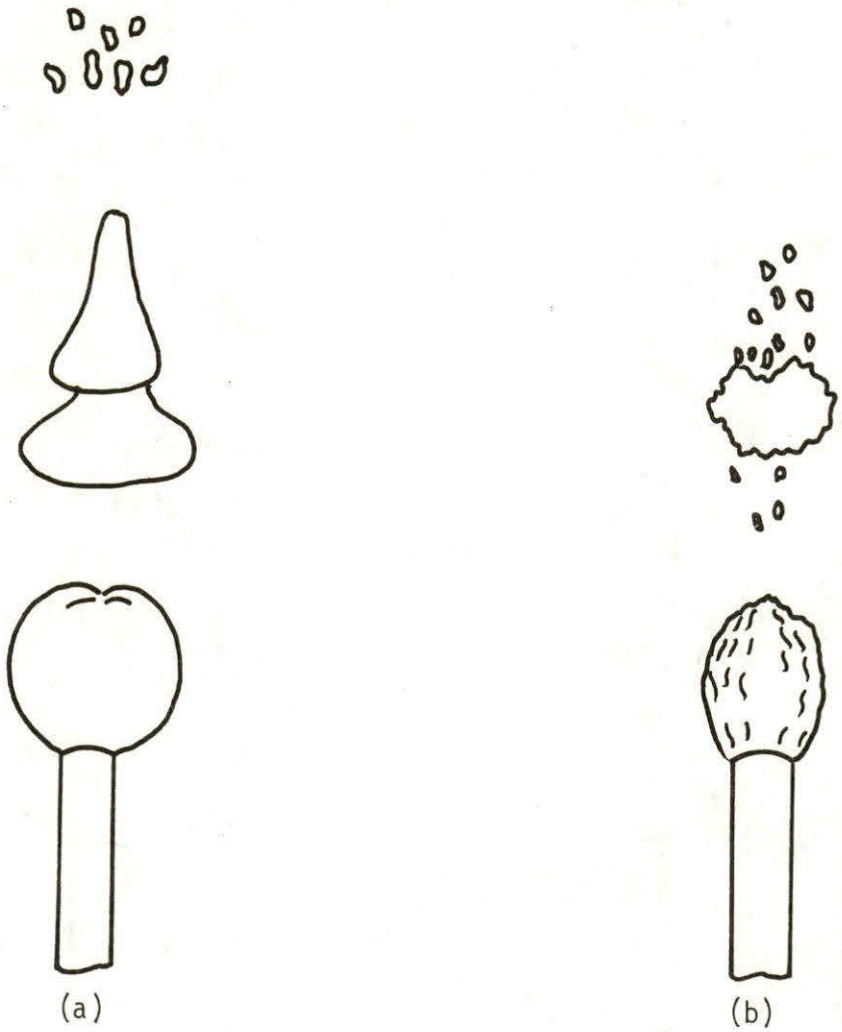

1.9 m/sec exit velocity

14 m/sec exit velocity

Fig. 3.2 Bubble formation at 0.64 cm diameter pipe exit.

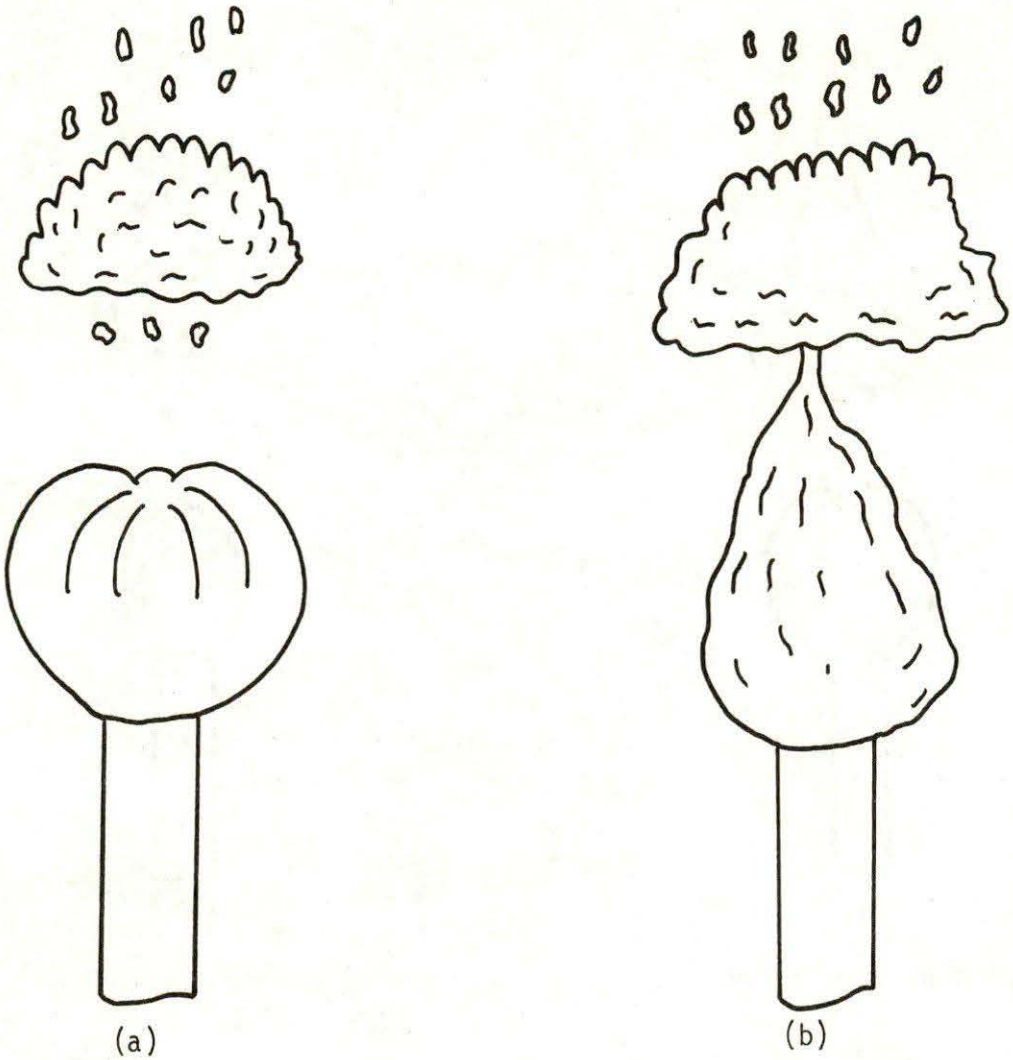

Fig. 3.3 Bubble formation at 2.2 cm diameter pipe exit.

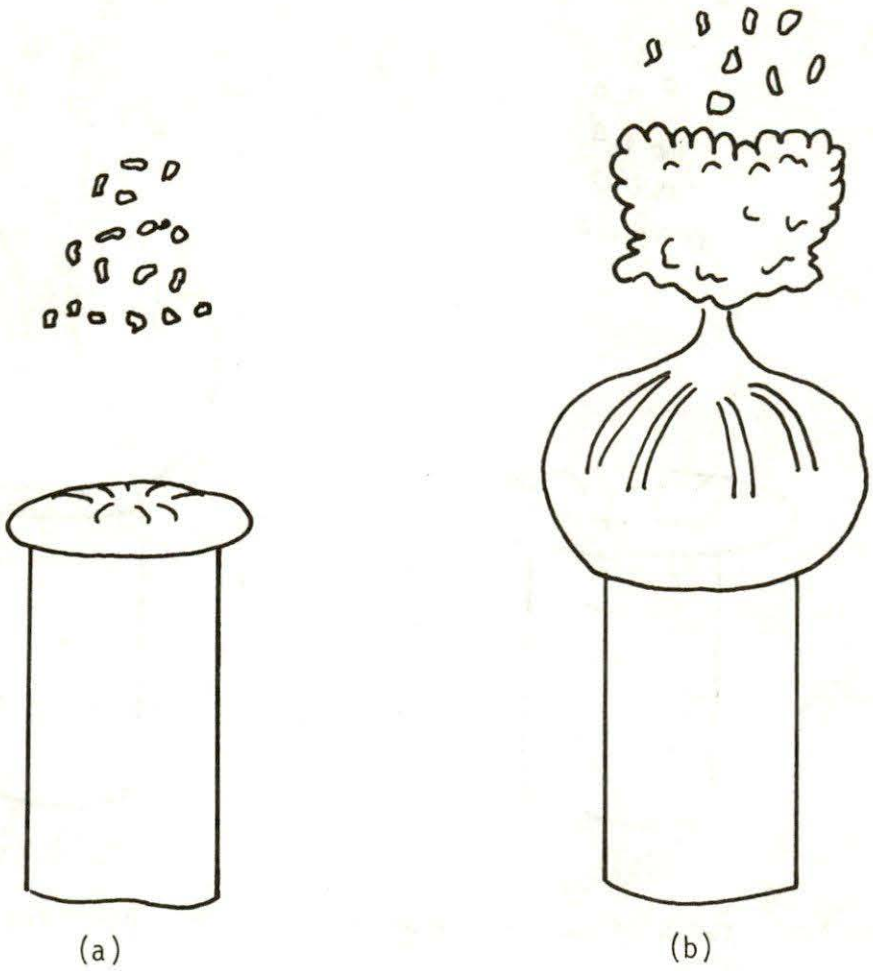

(a) Initial stages of bubble formation

(b) Near breakaway

Fig. 3.4 Formation of bubbles at 7.6 cm diameter orifice with 1.9 m/sec gas exit velocity.

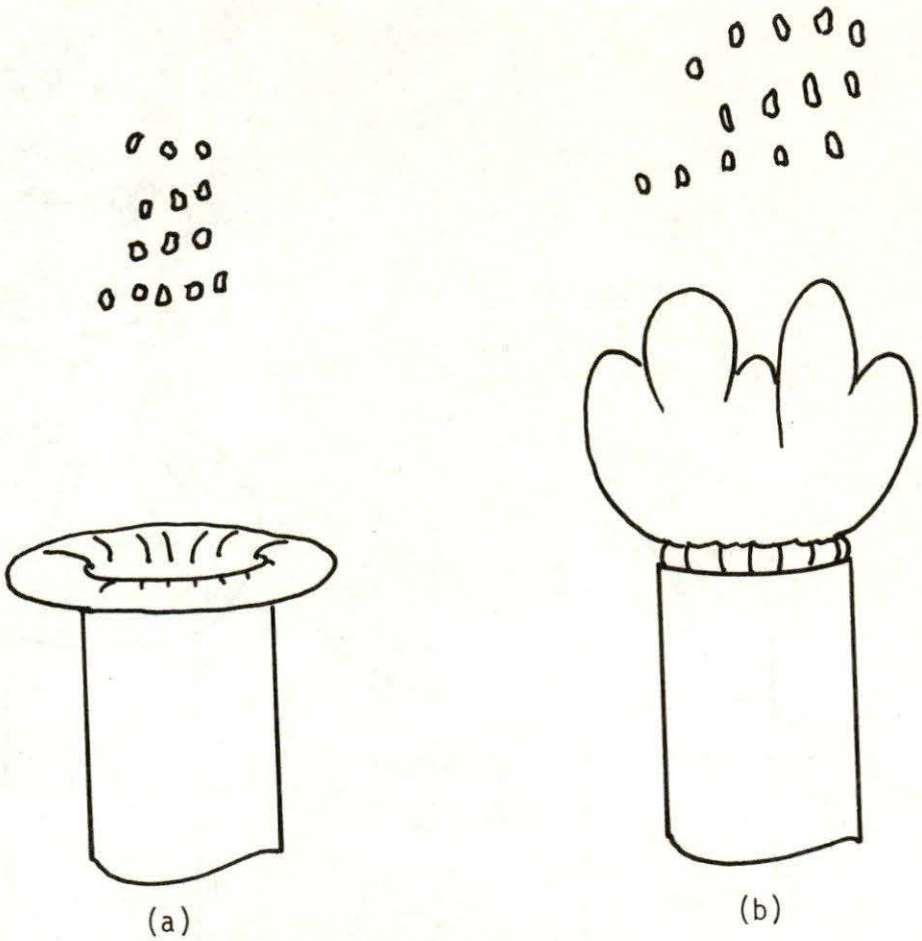

Initial stages of bubble formation

Near breakaway

Fig. 3.5 Formation of bubbles at 14.7 cm diameter orifice with 1.9 m/sec gas exit velocity.

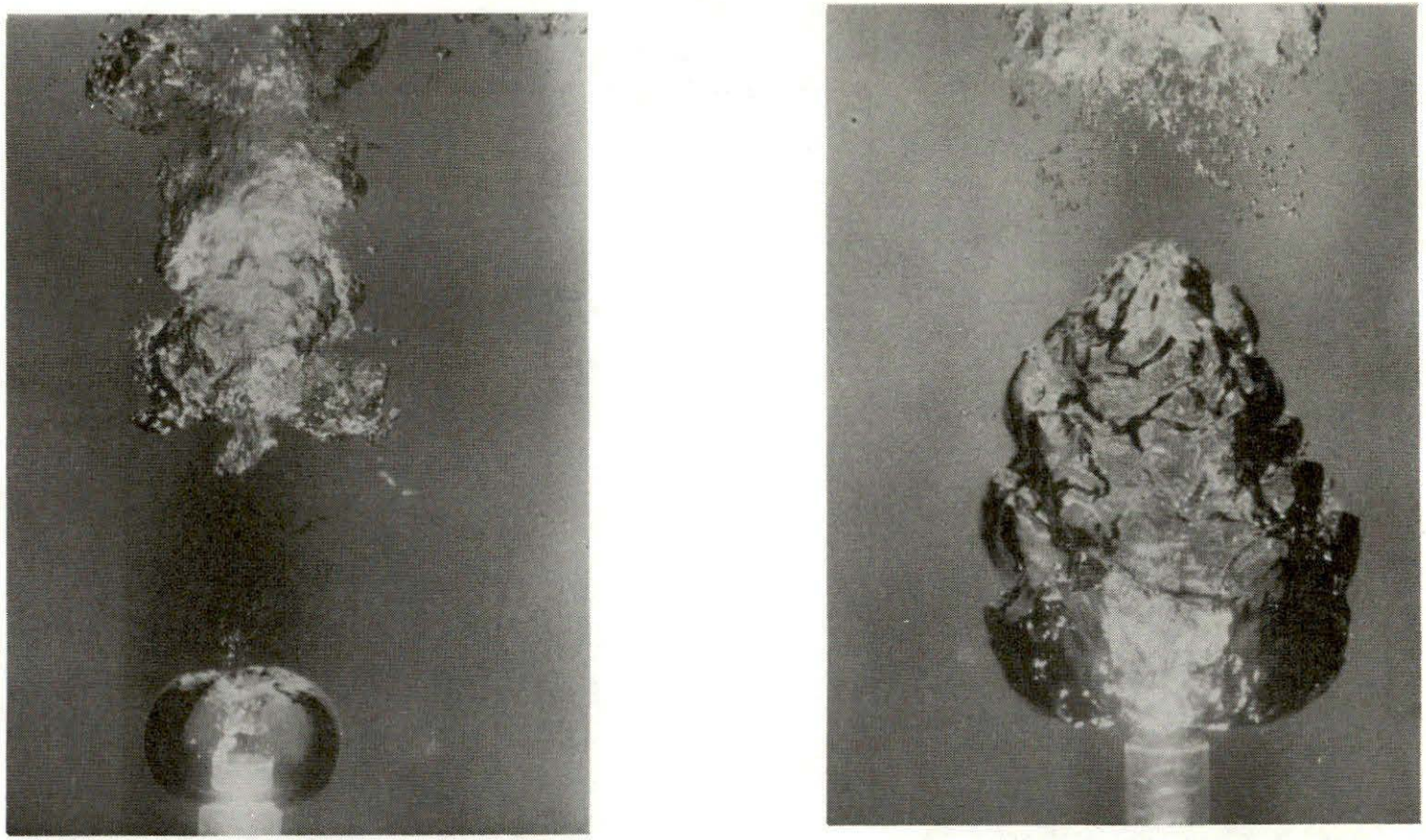

(a) (b)

Fig. 3.6 Nitrogen injected into water, exit velocity (a) 1.9 m/sec, (b) 14 m/sec.

(a)

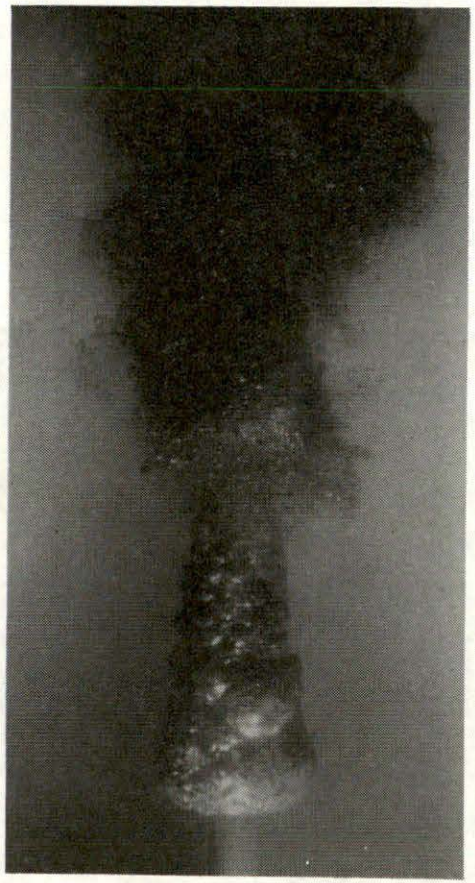

(b)

Fig. 3.7 Nitrogen plus Norman Wells crude injected into water, exit velocity (a) 1.9 m/sec., (b) 14 m/sec.

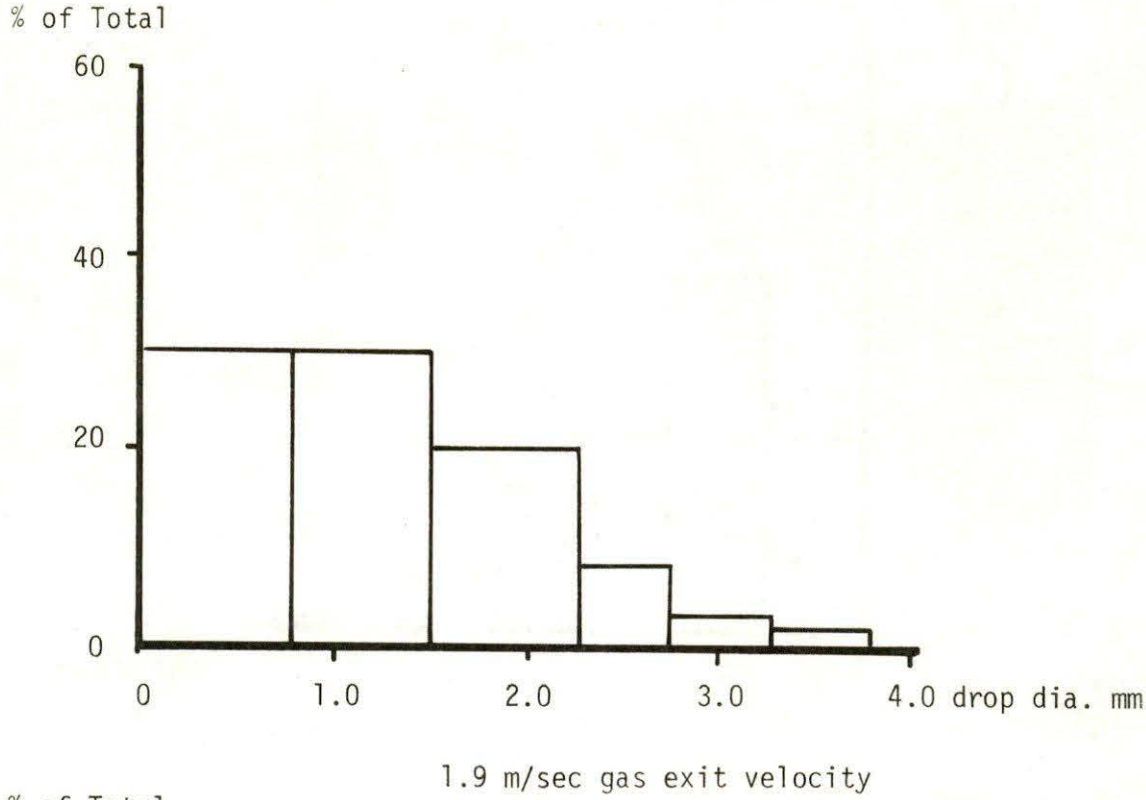

1.9 m/sec gas exit velocity

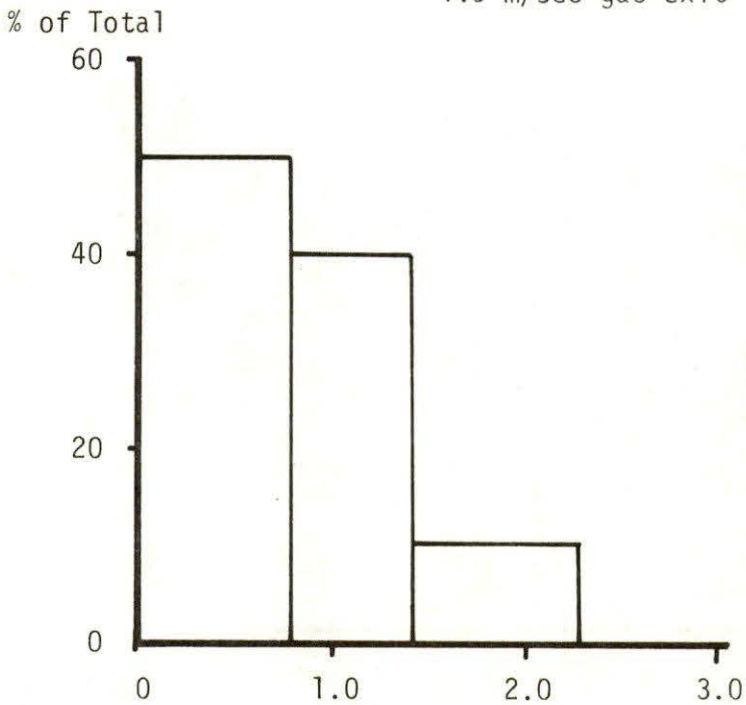

14 m/sec gas exit velocity

Fig. 3.8 Injection of Norman Wells crude into fresh water, 0.64 cm diameter pipe.

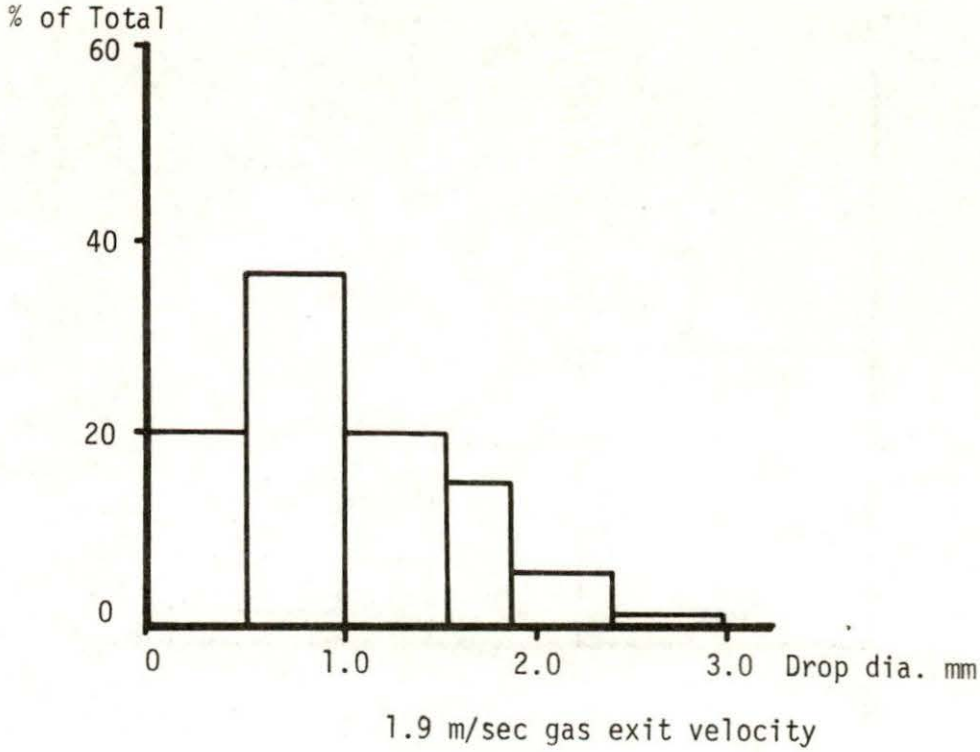

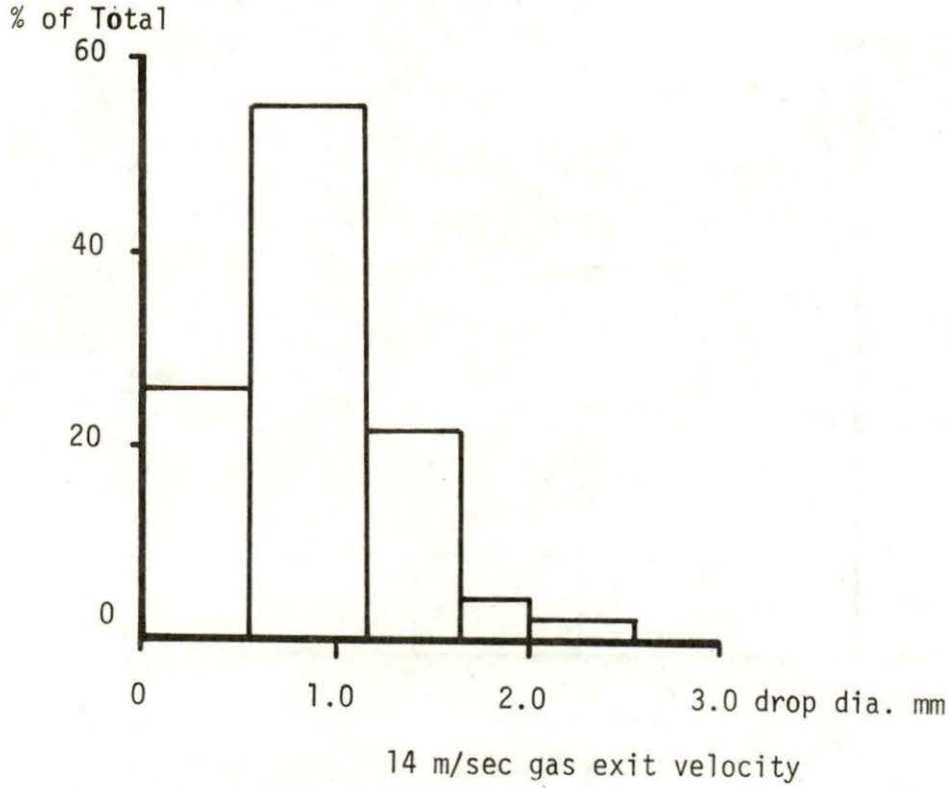

Fig. 3.9 Injection of Norman Wells crude into fresh water, 2.2 cm diameter pipe.

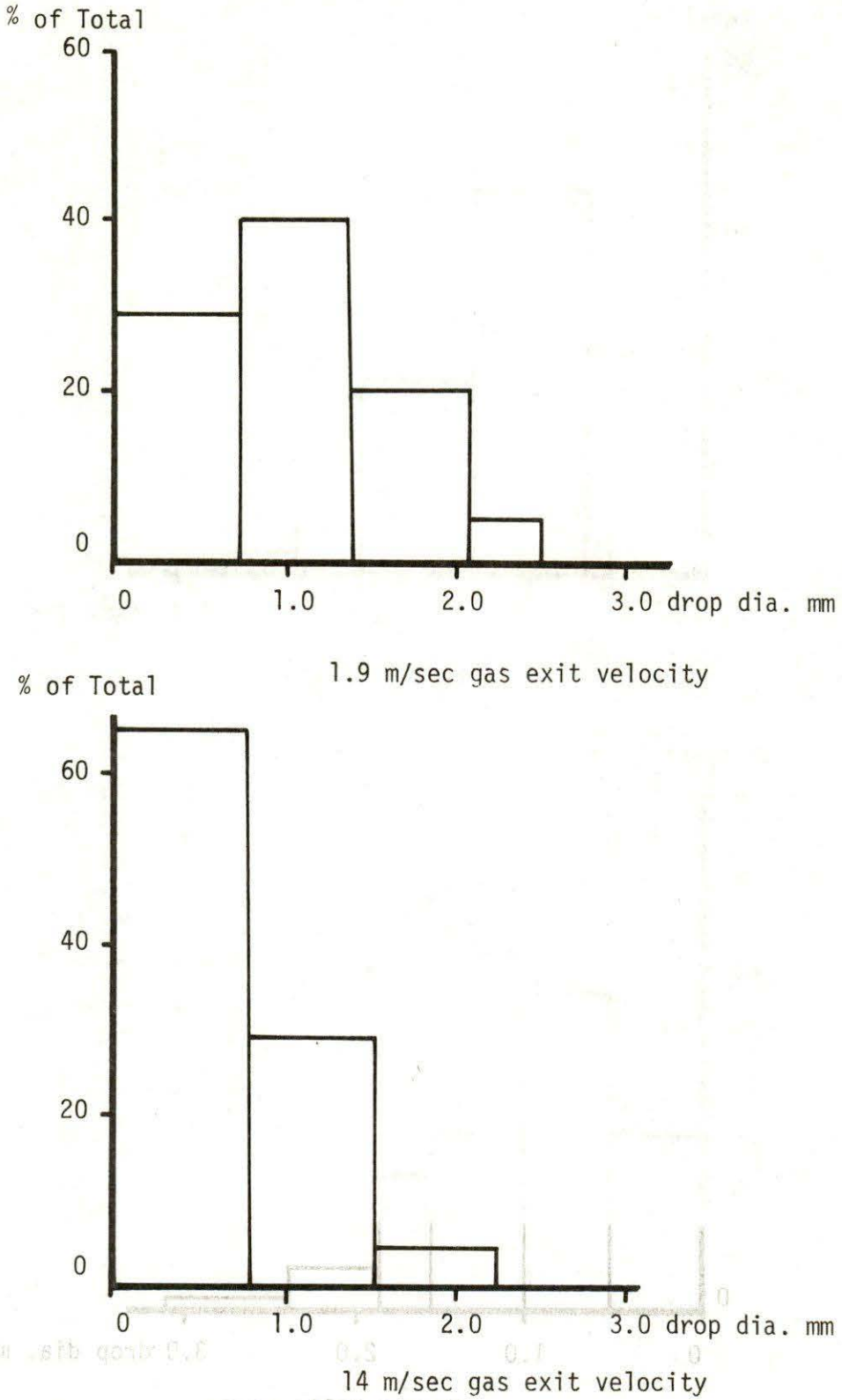

Fig. 3.10 Injection of Norman Wells crude into sea water, 2.2 cm diameter pipe.

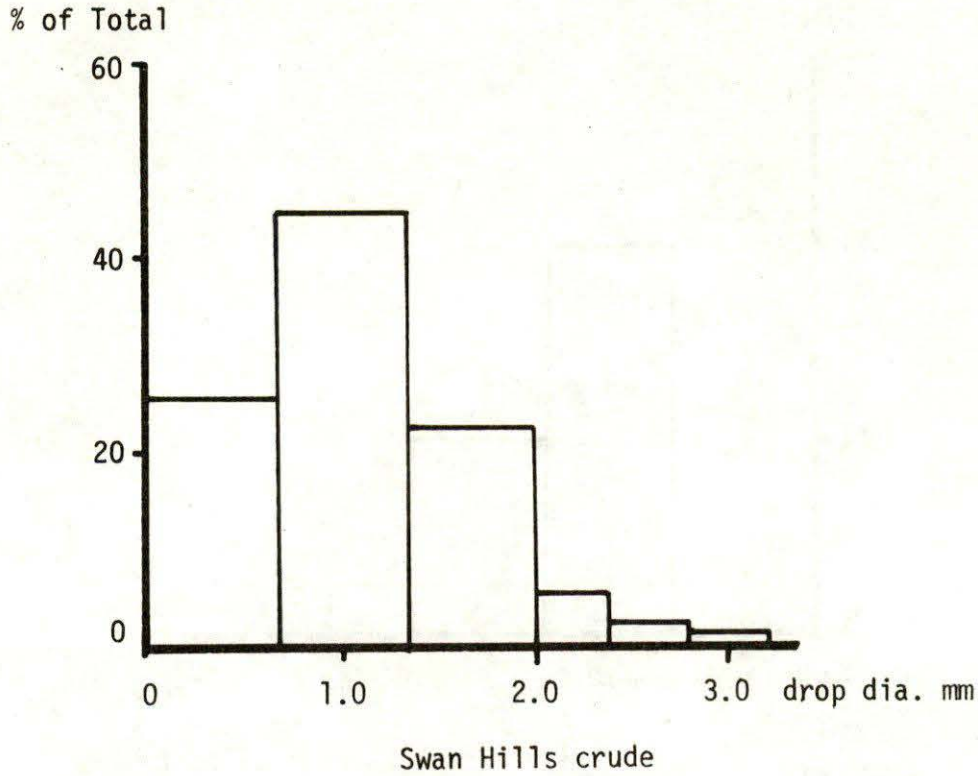

Swan Hills crude

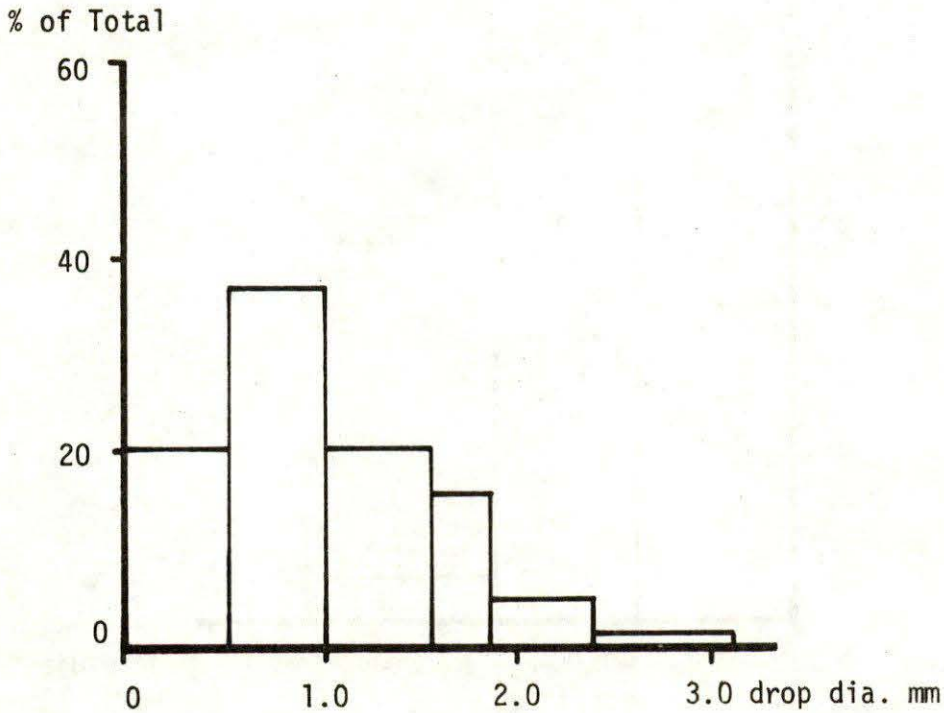

Norman Wells crude

Fig. 3.11 Injection of crude oils at a gas velocity of 1.9 m/sec into fresh water, 2.2 cm diameter pipe.

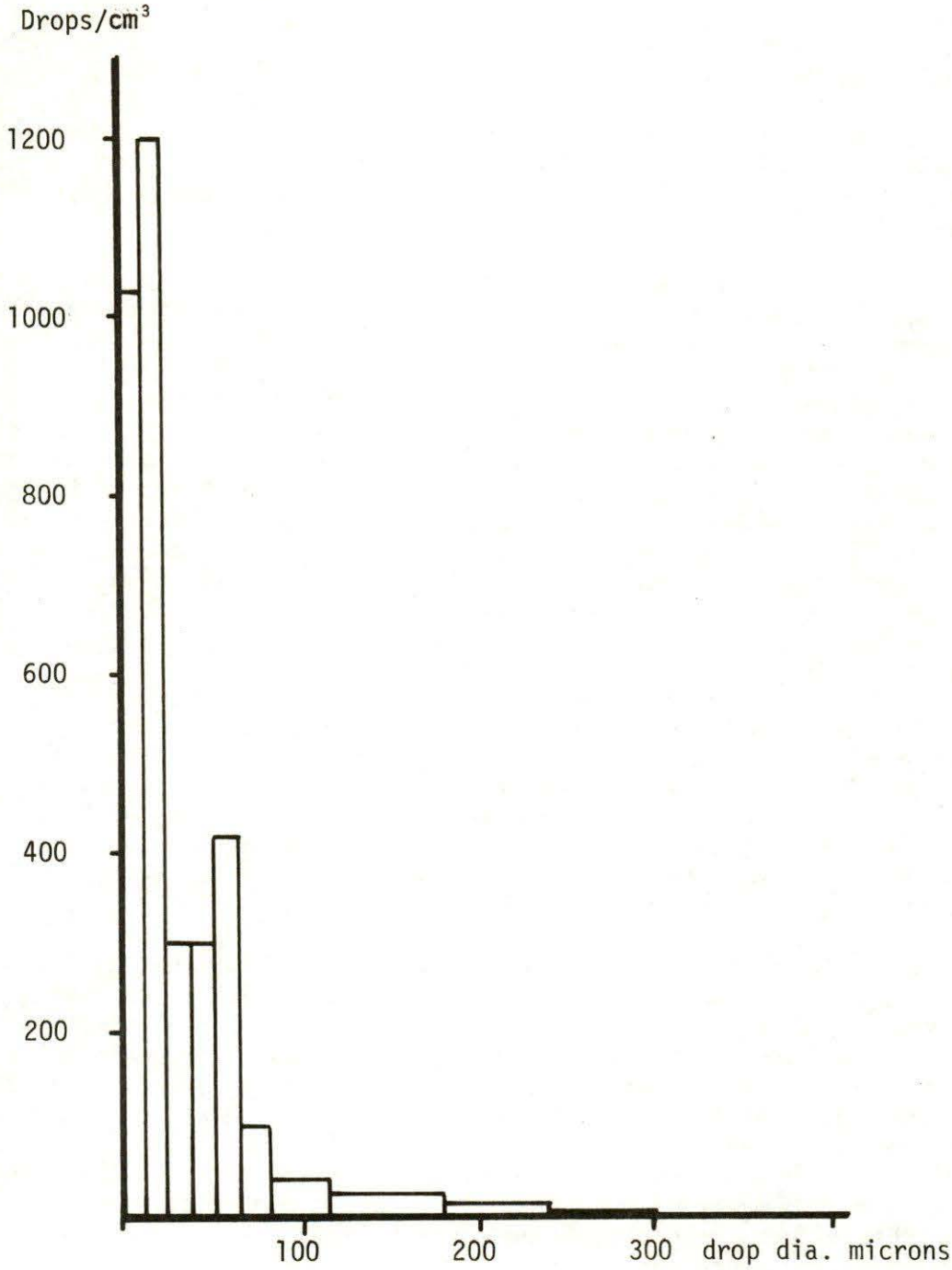

Fig. 3.12 Swan Hills crude injected into fresh water with 1.9 m/sec gas exit velocity, 2.2 cm diameter pipe.

4. THE BLOWOUT SCENARIO

The results obtained from the experiments described in Sections 2 and 3 can be combined to give a description of the likely consequences of an undersea oil well blowout. The conditions assumed for the oil and gas flow are those of the 'standard Beaufort Sea blowout' of the introduction, i.e. 2500 barrels/day (398 m^3/day) reducing to 1000 barrels/day (159 m^3/day) after one month, thereafter memaining constant. A constant gas content of 22.7 m^3/barrel when expanded to atmospheric pressure is assumed.

The general effect of such a blowout is a rising mixture of oil droplets and gas bubbles which entrain the surrounding water to form a buoyancy driven plume. The oil flow rate in the present case is less than 1% of the gas flow and its contribution to the total buoyancy can be considered negligible. However, the oil may have a secondary effect on the plume in that a film of oil on the gas bubbles may modify the effective surface tension and influence their behaviour.

The large scale bubble plume experiments carried out in water depths of 23 and 60 m showed that these plumes are not well described by existing theoretical models and thus the results cannot be extrapolated to deeper water depths with confidence. The main departure of the results from simple plume models is that they are initially conical in shape and then at some height become cylindrical with no great changes in vertical water velocity with height. The initial angle of expansion and the height of transition to the cylindrical form appear to be functions of the gas flow rate or, as the bubble volume changes with height, of the ratio of bubble volume flow to entrained water volume flow. The greater depth of water considered for the Beaufort Sea study well blowout is 180 m, beyond the range of the present experiments, however a tentative picture of plume shape has been drawn based on the measured entrainment rates and gas/water flow rates.

The probable plume shapes for depths of 15, 60 and 180 m of water with the specified flow rate of 40 m^3/min of free gas are shown in Figures 4.1, 4.2 and 4.3. For the 180 m depth, the relative bubble volume increases rapidly over the last 60 m and since comparison with the measured low gas flow plumes suggests that regions below that may be mainly cylindrical, the surface interaction flows have been scaled from a virtual origin at the 60 m depth.

It was suggested in the interim report, Topham 1974, that with a plume in a stably stratified environment, fluid may be shed from the sides of the plume. Heavier fluid is lifted to higher levels by the entrainment of the rising bubbles, and as far as the water alone is concerned, it is in an unstable condition with respect to the surrounding water. If this escapes from the influence of the bubbles it will descend to some equilibrium level. An unpublished work in Cambridge, England (T. J. McDougall, private communication) with a small plume in a stratified tank confirms this view. However at this time no criterion for critical density gradient for this effect to be significant is available. This is an important consideration where the oil is in droplets small enough to be carried with such flows, and thus to be released from the plume deep in the ocean. If any changes in gas bubble behaviour due to the presence of the oil are

neglected, the buoyant plume acts merely to transport the oil from the sea bed to the surface.

The oils selected for the injection studies are considered to represent the extremes of the oils expected in the Beaufort Sea, and represent an oil which might form stable emulsions (Swan Hills crude) and one which would not (Norman Wells crude). The nature of the flow of the oil and gas mixture within the exit pipe is largely determined by their relative volumes, and for the conditions assumed here range from a 'slug' flow of alternating regions of gas and oil, through a 'froth' flow to an annular flow of oil surrounding the gas flow at high exit velocities.

In the injection experiments the oil was broken into a wide range of droplet sizes, with diamaters from 3 mm downwards, a limit of 15 microns being set by the measurement techniques. The bulk of the oil volume was contained in the range 0.5 to 1 mm diameter. The higher gas injection velocities gave a shift towards the smaller sizes. The main mechanisms of droplet formation appeared to be centred in the region close to the pipe exit where released gas bubbles shattered into small fragments. The higher the gas flow rate the greater the fragmentation. It was not possible to determine whether or not the state of the oil flow within the pipe strongly influenced the droplet distributions. The natural rise velocity of 1 mm oil drops is small compared with the vertical water flows of 60 cm/sec measured in the plume experiment. If the total oil flow is considered to be in 1 mm diameter droplets distributed throughout the rising water column, a mean density of less than 1 drop/cm^3 is obtained, and it is unlikely that any coalescence would take place within the rising column. Drops of this size have a natural rise velocity of the order of 5 cm/sec and if they were swept by the radial current to depths of 3m would rise to the surface at a distance of 18 m, well within the wave ring. The oil would be swept out to the wave ring and after exceeding some critical depth would escape and then accumulate in an annular ring beyond this.

Related studies of oil trapped under ice show that the oil accumulates in sessile drops approximately 0.8 cm thick. If it is assumed that the undersurface of the ice is perfectly flat, this 0.8 cm minimum thickness can be used to place upper limits on the area directly contaminated by the oil. Three simple situations can be considered, that the area within the wave ring is ice free and oil is contained within this volume, that it has a stationary ice cover, or has a steadily moving ice cover, an oil thickness of 0.8 cm being assumed in the two latter cases. Figure 4.4 shows the rise of oil with time within a volume enclosed by the wavering, Figure 4.5, the increase in the outer radius of an annulus of oil growing under a stationary sheet of flat ice, and Figure 4.6, the width of the trail of oil left behind on a moving continuous ice sheet. This last curve is derived from simple considerations of continuity based on the initial flow rate of 2500 barrels/day.

A small proportion of the oil, of the order of 1%, may be in droplets 50 microns in diameter or less, these have a natural rise velocity of 0.5 mm/sec. It is probable that drops of this size would be swept down to depths of 10 m at the wave ring and if released at this depth, would travel several kilometres during their rise to the surface.

The capacity of a bubble driven plume to raise warm lowlying water to the surface and hence alter the heat balance at the ice/water interface is often exploited to maintain waterways open to shipping. The operation of such systems has been studied by Ashton, 1974, the heat transfer between the water and the ice being deduced from measurements on impinging heated air jets. Experiments on actual ice/water bubbler systems subsequently confirmed these predictions (Ashton, 1975).

Combining these heat transfer measurements with the simulated blowout results enables an estimate to be made of the melting of the ice cover. Consider a layer of warm water of thickness Δhm lying on the bottom in water of h meters depth. The rising plume entrains water continuously from its surroundings, and the water temperature within the plume attains some value between that of the original warm layer and the main body of the ocean. The rate of entrainment of fluid by the plume was found to vary rather erratically with height and for the present purpose a constant mean value of 8.4×10^4 gm/sec cm will be taken. Taking Ashton's heat transfer data, and assuming that all the heat transferred to the ice goes towards melting, over a 20 meter diameter circle, with a water impingement velocity of 0.7 m/sec the rate of ice melt can be written as

$$\frac{d\eta}{dt} = 21\ \Delta T_s \text{ cm/day}$$

where η is the ice thickness and ΔT_s is the temperature difference between the melting temperature of ice and the impinging water column. With the assumption of a constant mass entrainment rate,

$$\Delta T_s = \frac{\Delta h}{h} \cdot \Delta T$$

For example, a 10 metre layer of water 0.5°C above the bulk temperature in 100 metres total depth gives a melt rate of 1.05 cm/day.

4.1 References

Ashton, G. D. Air bubbler systems to suppress ice. Corps of Eng. U.S. Army. Cold Regions Research & Eng. Lab, Hanover, New Hampshire, USA, Special report 210, Sept. 1974.

Ashton G. D. Experimental evaluation of bubble - induced heat transfer coefficients. Third International Symposium on Ice Problems, Hanover, New Hampshire, USA

Topham D. R. The hydrodynamic aspects of an oil well blowout under sea ice. Interim Report, Beaufort Sea Project, Dec. 1974, Dept. of Environment, Victoria, B.C.

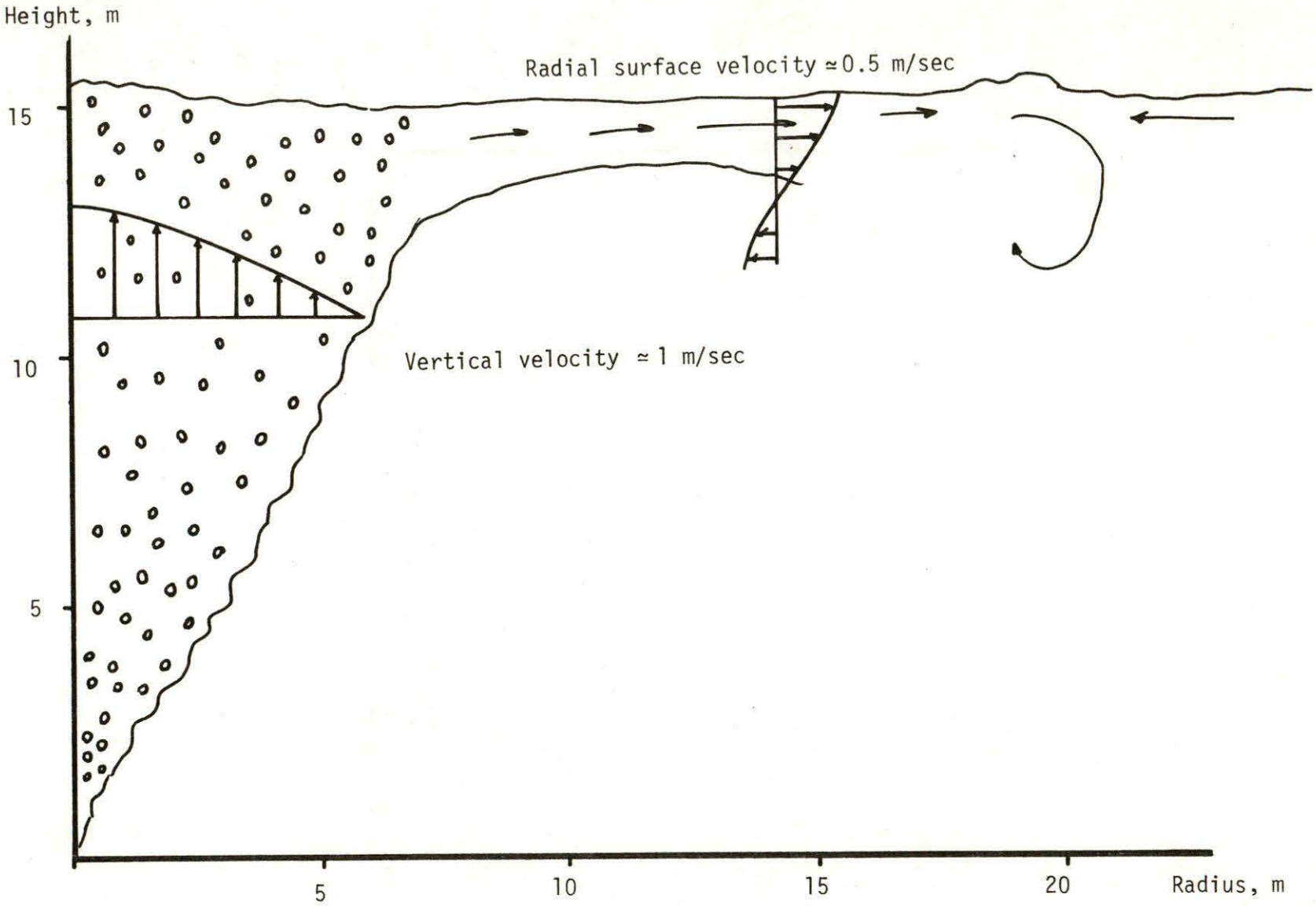

Fig. 4.1 Plume Shape, 15 m depth.

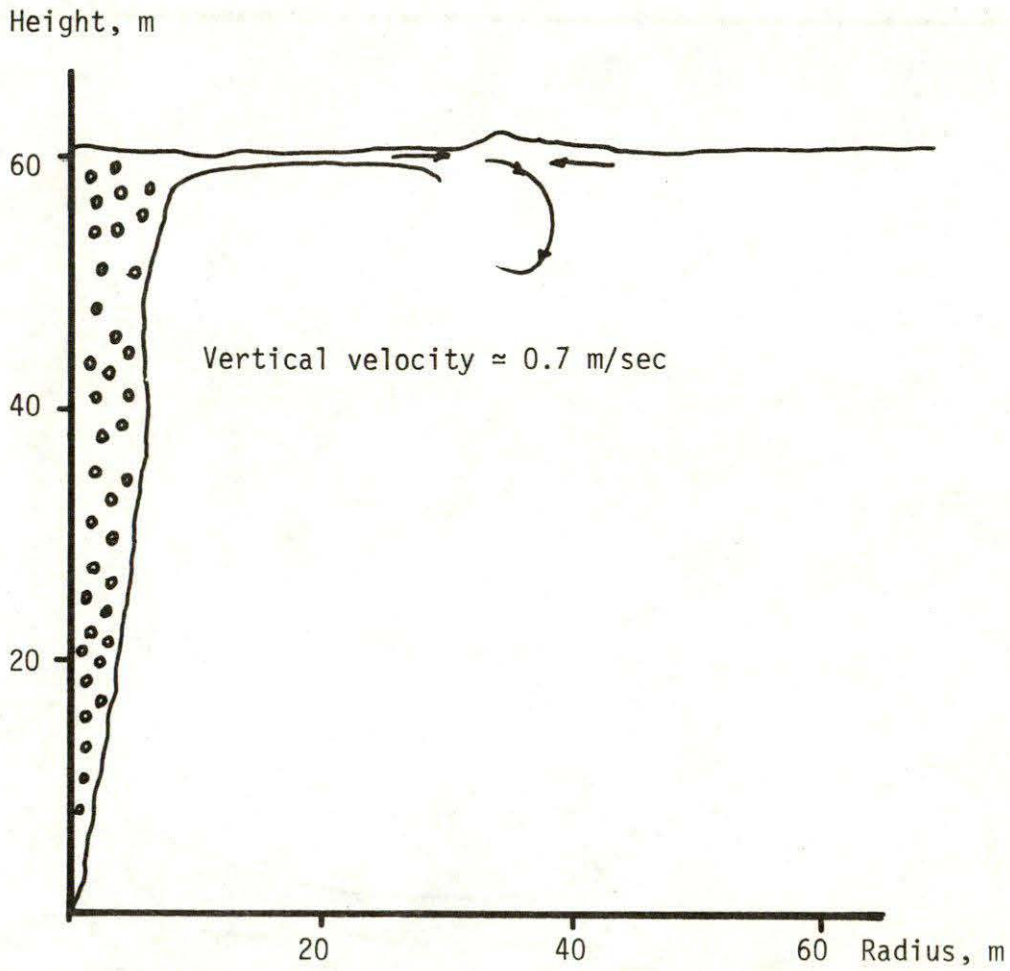

Fig. 412 Plume Shape 60 m depth.

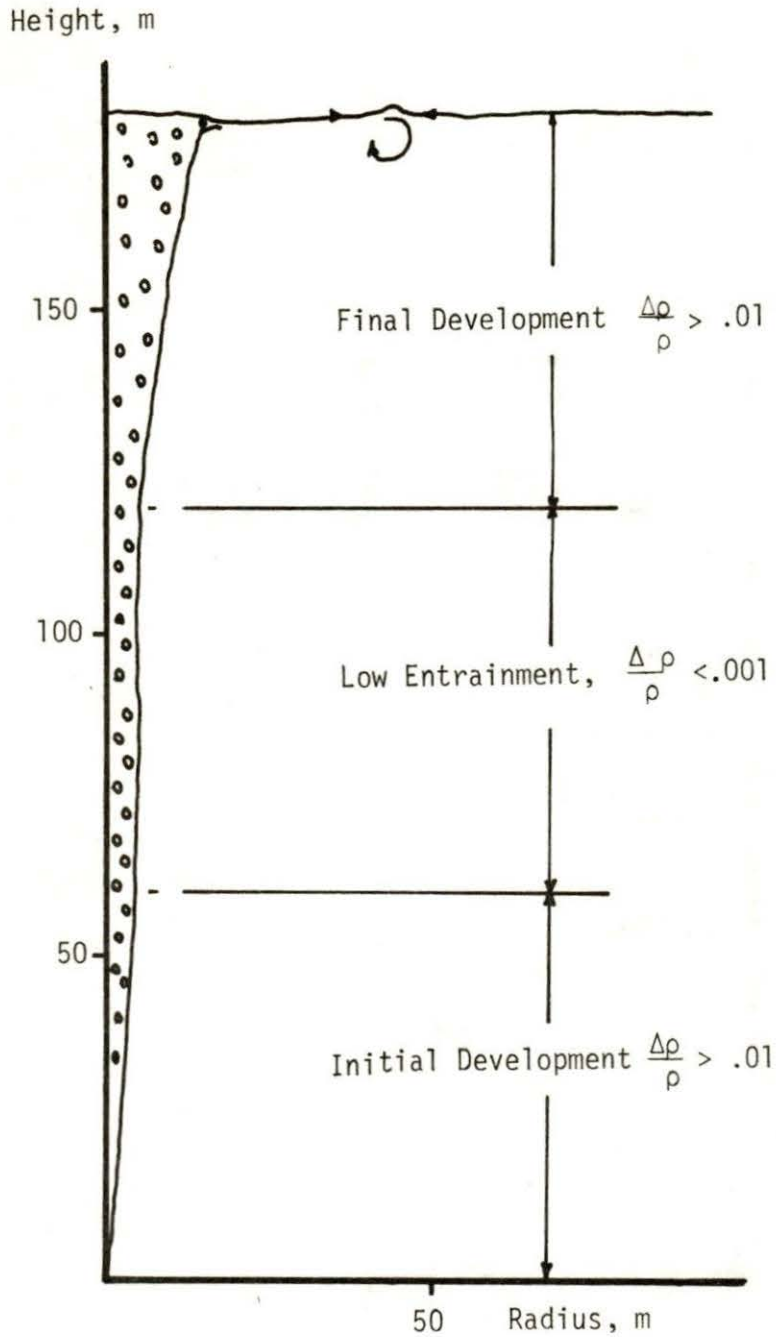

Fig. 4.3 Plume Shape, 180 m depth.

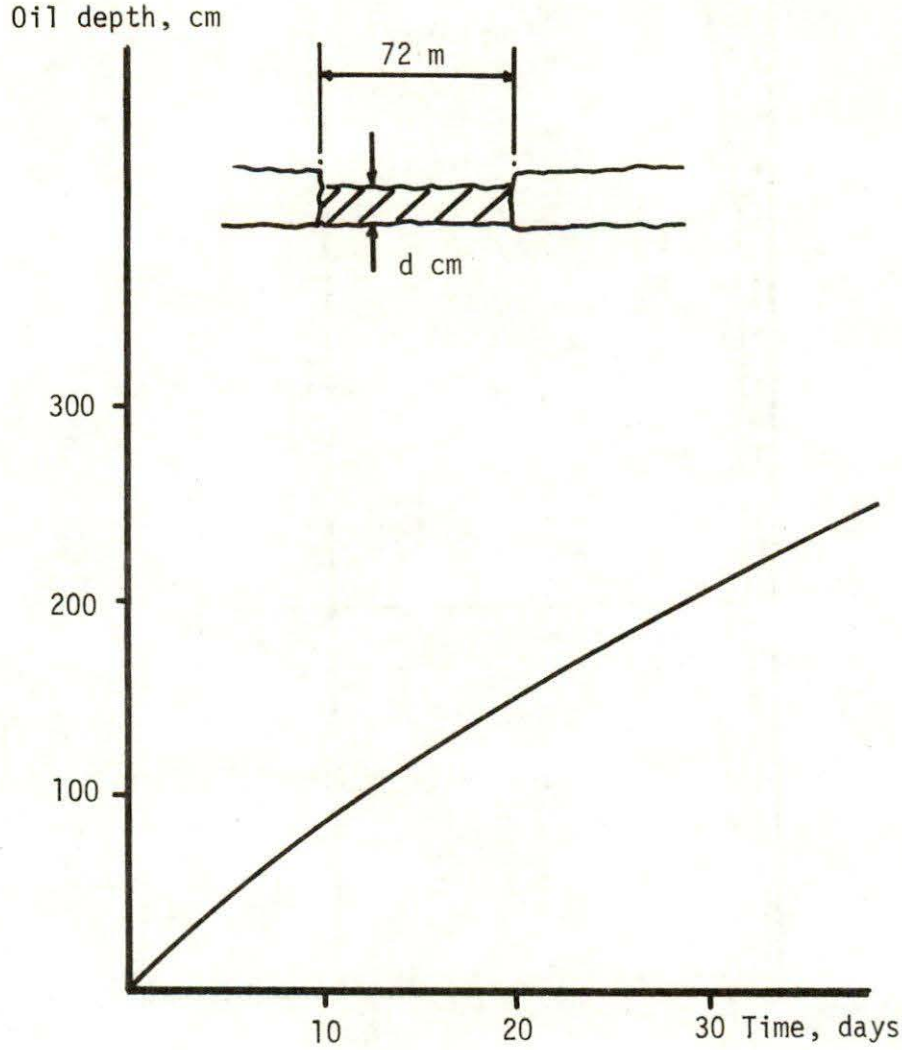

Fig. 4.4 Oil depth, open water containment, 60 m water depth.

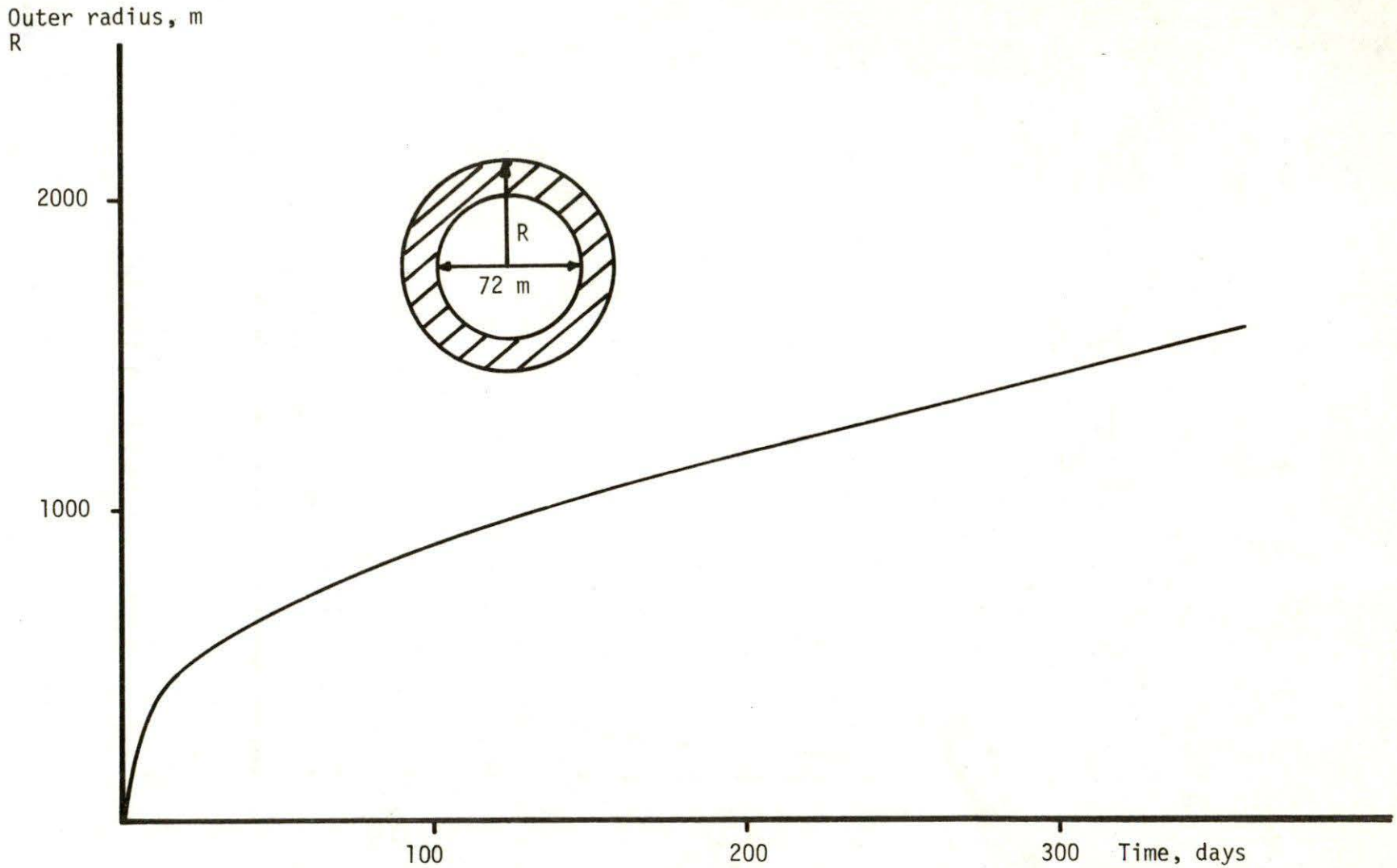

Fig. 4.5 Radius of contaminated area as a function of time for sessile drop thickness of 0.8 cm.

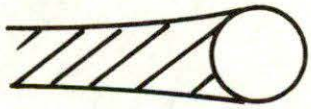

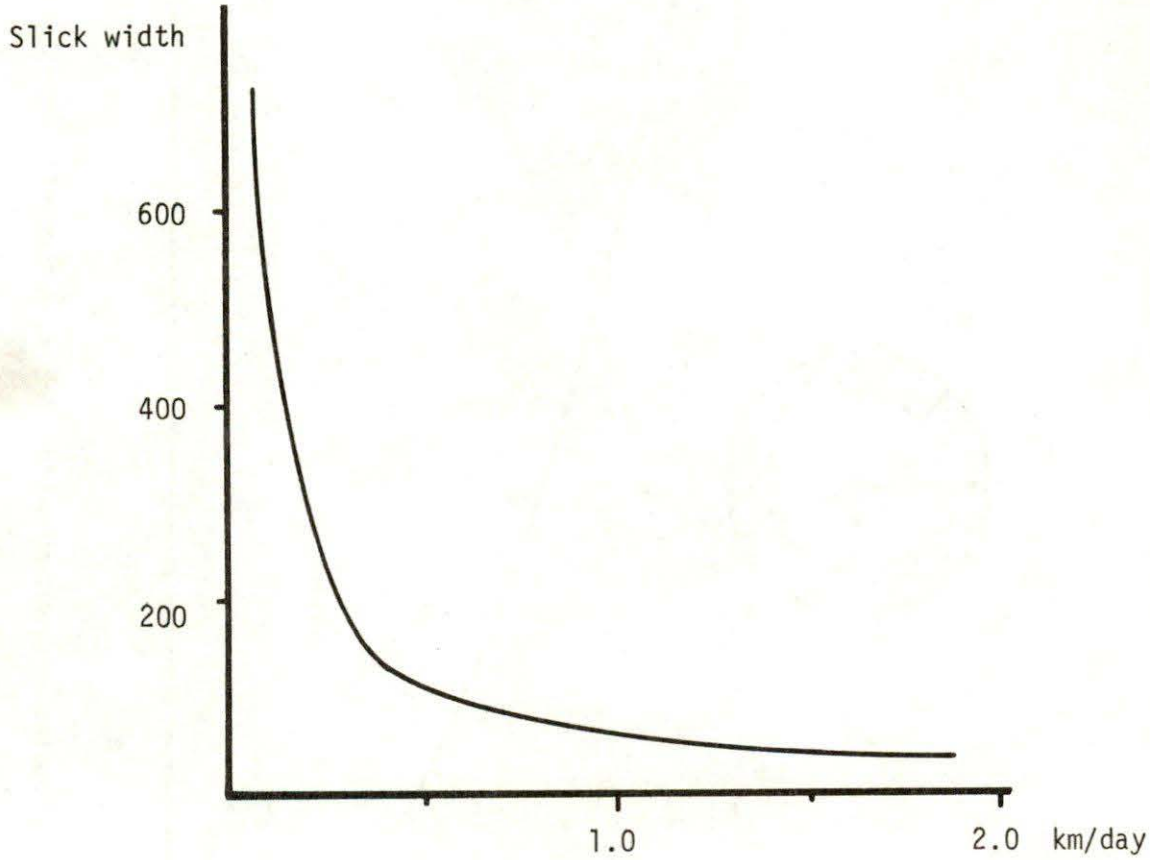

Fig. 4.6 Slick width, moving ice cover for oil discharge of 2500 barrels/day and 0.8 cm thickness.